NPS ARCHIVE
1958
GOSLOW, P.

INVESTIGATION OF A RELAY SERVO USING A SERIES MOTOR

PAUL GOSLOW

LIBRARY
U.S. NAVAL POSTGRADUATE SCHOOL
MONTEREY, CALIFORNIA

8854

INVESTIGATION OF A RELAY SERVO USING A SERIES MOTOR

* * * * *

Paul Goslow

INVESTIGATION OF A RELAY SERVO USING A SERIES MOTOR

by

Paul Goslow

Lieutenant, United States Navy

Submitted in partial fulfillment of
the requirements for the degree of

MASTER OF SCIENCE
IN
ELECTRICAL ENGINEERING

United States Naval Postgraduate School
Monterey, California

1 9 5 8

NPS ARCHIVE
1958
GOSLOW, P.

INVESTIGATION OF A RELAY SERVO USING A SERIES MOTOR

by

Paul Goslow

This work is accepted as fulfilling

the thesis requirements for the degree of

MASTER OF SCIENCE

IN

ELECTRICAL ENGINEERING

from the

United States Naval Postgraduate School

ABSTRACT

The series motor has had limited use in servomechanisms eclipsed no doubt by other motors that allow linear techniques to be used in the system design although its high starting torque could be used to great advantage in many applications.

As the motor component of a relay servo system the series motor, particularly those with split fields, accentuates the desirable characteristics of a relay system by providing maximum torque for starting and reversal. An investigation on an experimental relay servo using a split field series motor was conducted to determine the nature of the system characteristics. Step function and frequency response tests are described and illustrated. Optimized control through the use of linear error rate switching was found to be possible and quite promising. The applications of a split field series motor relay system include the possible replacement of expensive and complex dual mode and non-linear control positioning systems.

The author wishes to express his appreciation for the assistance and encouragement given him by Professor George J. Thaler of the U. S. Naval Postgraduate School in this investigation.

TABLE OF CONTENTS

Section	Title	Page
1.	Historical Background	1
2.	The Experimental Test System	7
3.	Mathematical Analysis	13
4.	Determination of System Parameters	21
5.	System Response to Error Control	33
6.	System Response to Error plus Error Rate Control	46
7.	Optimized Control	57
8.	The Effect of Inertia Loading	66
9.	System Response to a Relay with a Dead Zone	71
10.	Summary and Discussion	76
11.	Conclusions and Recommendations	79
12.	References and Bibliography	82

LIST OF ILLUSTRATIONS

Figure		Page
1.	Block Diagram of the Test System	8
2.	Schematic Diagram of Relay-Rectifier Unit	9
3.	Schematic of Control Amplifier Connections	11
4.	Schematic of the Test Set-Up	12
5.	Essentials of an Analogue Computer Solution	16
6.	Torque Speed Characteristics of the Test Motor	22
7.	Variation of Torque with Armature Current	23
8.	Variation of Torque with Terminal Voltage	25
9.	Determination of Inertia with Added Inertia Disks	26
10.	Tachometer Calibration	27
11.	Determination of Coulomb and Viscous Friction	29
12.	Switching Characteristics of the Relay-Rectifier	32
13.	Transient Response to Error Control	34
14.	The Effect of Signal Amplitude on Transient Peak Overshoot	35
15.	Phase-Plane of Error Controlled Response	36
16.	Frequency Response with Error Control	38
17.	M-N Contour Plot of Error Control	39
18.	Open loop Response of Error Control	40
19.	Polar Plot of Error Control	42
20.	Variation of Resonant Frequency and Magnitude	43
21.	Variation of M_p/f_r with Signal Amplitude	45
22.	The Effect of Error Rate Control on the Switching Line	46
23.	Phase-Plane of Error Rate Response	48

Figure		Page
24.	Transient Response to Error Rate Control	49
25.	The Effect of Error Rate Control on Peak Overshoot	50
26.	Frequency Response to Error Rate Control	51
27.	Variation of Peak Magnitude with Error Rate Control	53
28.	M-N Contour Plot of Error Rate Control	54
29.	Open Loop Response of Error Rate Control	55
30.	Polar Plot of Error Rate Control	56
31.	Phase-Plane of Optimum Control	58
32.	Transient Response with Optimum Control	60
33.	Frequency Response of Optimum Control	61
34.	M-N Contour Plot of Optimum Control	62
35.	Open Loop Response of Optimum Control	63
36.	Polar Plot of Optimum Control	64
37.	The Effect of Inertia on Transient Response	67
38.	The Effect of Inertia in the Phase Plane	68
39.	Optimum Switching with Added Inertia	69
40.	The Effect of an Open Dead Zone on the Phase-Plane Response	72
41.	Transient Response with an Open Dead Zone	74
42.	Optimum Switching with an Open Dead Zone	75
43.	Proposed Grid Control Circuit	78

TABLE OF SYMBOLS

Symbol		Units
C	Coulomb friction	oz-in
J	Inertia	$oz\text{-}in^2$
K	Constant of proportionality	
L	Inductance	heneries
R	Resistance	ohms
V	Motor terminal voltage	volts
f	Viscous Friction	oz-in/deg/sec
i	Armature Current	amperes
θ	Angular position	degrees
$\dot{\theta}$	Angular velocity	deg/sec
$\ddot{\theta}$	Angular acceleration	deg/sec^2
$\mathcal{E}$	Error	degrees
$\dot{\mathcal{E}}$	Error rate	deg/sec
$\ddot{\mathcal{E}}$	Error acceleration	deg/sec^2
δ	Unit of delta construction	degrees

Subscripts

C	Controlled output
R	Reference input
b	Back e.m.f.
c	Output shaft
m	Motor shaft
t	torque

1. Historical Background

The simplicity of a relay servomechanism recommends itself for use in systems where cost or simplicity per se are the important considerations, particularly so in expendable devices such as guided missiles and torpedoes. Many aircraft positioning devices such as wing flap and landing gear actuators are relay controlled. In general they are used where continuous control is not required or where it may be approximated by continual relay action.

A relay servomechanism is characterized by a restoring force being brought into play when the output deviates a set amount from the input command. The restoring force is usually the maximum output of the driving unit which may vary during operation. The on-off nature of this type of mechanism is called discontinuous or non-linear according to the educational background of the person concerned (1), but in any event the equations of motion that describe the system do not yield a continuous solution. Hazen (2) used ordinary linear methods piecewise to solve a constant torque system and later Weiss (3) solved the same system using phase plane methods. The literature provides an abundance of numerical, analogue, describing function, and other methods of solution for relay systems. Hopkin's phase plane analysis (4) was conducive to his definition of an optimum relay-servo, viz: a relay servomechanism which drives at full torque to reduce the difference between the output and the reference until such a time that when full reverse torque is applied, the system will decelerate

to a stop at the desired position. The system he used in obtaining data involved determining the character of the non-linear elements, plotting this as a boundary curve and then controlling the system with a curve reading device. In this case a mask over the face of an oscilloscope exposed the boundary region to a phototube which controlled the relay operation. Goldfarb (5) described a harmonic balance method in which he defined an equivalent input admittance of a non-linear element as a complex function. This method was used by Lechtman (6) to particularly describe relay systems with greatly reduced labor, however the method is quite approximate in character.

The direct current series motor has been used for many years in applications requiring large starting torques such as in electric trolleys and trains, rolling mills, gyro-stabilizers, and lately in radar systems. In these applications the loads were either high inertia or high initial friction. In a servo-system a split field series motor has control and torque characteristics quite similar to those of a two-phase induction servo-motor and it provides the high starting torque in a d.c. system that the induction motor does in an a.c. system. The time constant of a series motor is, however, of little use in a mathematical analysis since it may vary as much as 10 to 1 from starting to steady state speed (7), hence the motor is non-linear to such a degree that an analysis using a linear approximation is not practical. The driving torque is proportional to the product of flux and armature current which are subject to non-linear magnetic saturation. In

the linear portion of the magnetization curve where flux is proportional to current, the torque may be assumed to be proportional to the square of current since the armature current flows in the field winding also, but a second degree term in a differential equation makes the solution extremely laborious, therefore, confining operation to the linear region does not greatly simplify the analysis.

As the driving unit of a relay-servo, this motor may be used to obtain maximum advantage of the characteristics of the optimum relay-servo as defined by Hopkin. In such a system a series motor would produce maximum initial acceleration, then at reversal the back e.m.f. would add to the reversed voltage with a combined effect of super-deceleration.

References in the literature to relay-servo systems using split field series motors are few and far between and these seldom mention any analysis. The systems were evidently built by trial and error methods avoiding the obvious difficulties of analyzing a non-linear motor coupled with the discontinuous controller.

Williams (8) described a null-type recorder using a split field series motor controlled by thyratron tubes acting as rectifier-relays. A motor driven square law tachometer produced a voltage which when subtracted from the error voltage of a potentiometer bridge controlled the cut-off of the thyratron tubes. The motor was driven at full torque to reduce the voltage difference to zero at which time the kinetic energy of the motor-load combination was equal to the energy that could be absorbed in

braking, and the motor was allowed to coast to the null position. The square law tachometer consisted of a non-linear copper-copper oxide rectifier used with a linear tachometer. This servo was also used as a high speed controller by employing any error detector that gave a voltage proportional to the error.

A water level indicator described by Ware (9) used a split field series motor to drive a pen and probe. The resistance of the probe just touching the surface of the water balanced a bridge which in turn controlled the firing of thyratron rectifier tubes. The motor ran at full torque driving the probe through a worm gear of such a large ratio that the decelerating low inertia motor did not provide enough unbalance in the bridge to fire the tubes.

Several aircraft applications of remote and automatic control described by Lear (10) included a number of relay-servo systems using split field series motors. Primarily positioning mechanisms, the motors were supplied directly from the aircraft d.c. system. The motors were driven at full torque in the appropriate direction to balance a potentiometer bridge which controlled the relay either directly or through vacuum tubes. A null-seeking device described used a Selsyn system in place of the bridge for an error indicator. Most of the Lear devices incorporated the Fastop clutch which disengaged the motor from the load, braked the load to a stop and held it stationary when the relays opened.

The Fairchild developed K-8 Computing Gunsight (11) of World War II used thyratrons as relay-rectifiers to control two split

field series motors that moved the mirrors of this offset-line-of-sight system. The sight was used in machine gun turrets of heavy bomber aircraft such as the B-17 Flying Fortress. An electronic computer calculated the azimuth and elevation leads required to properly hit an attacking aircraft and sent command voltages to a sensitive (20mv) d.c. amplifier which in turn controlled the firing of the thyratron tubes. The plates of the thyratrons were supplied from a four phase alternator with the tubes providing on-off half-wave rectification for each field of the two motors. In addition to driving the offset mirrors, the motors powered permanent magnet generators which supplied a speed voltage to both the computer and a bucking potentiometer. When the difference between the error voltage and the bucking potentiometer was reduced below the sensitivity of the d.c. amplifier the thyratrons ceased firing. The potentiometer was set by the operator just below that point where oscillations occurred, thus selecting the maximum response for this system. In the condition of worst sensitivity (40mv) of the d.c. amplifier the system had an accuracy of 2 yards at 1000 yards, well within the accuracy of the guns themselves.

Macon Fry described several relay-servo systems in his paper on Computing Mechanisms (12) including some driven by split field series motors. These systems incorporated a tachometer anticipation of the final position and cut off the power at the appropriate lead time. The tachometer produced a voltage proportional

to the speed of the motor which together with error magnitude gave the lead required. With the power off the motor slows, the lead diminishes proportionally and should just cancel the movement of the coasting motor. A slight over-lead was desirable, giving the system a series of small nudges toward the final position during deceleration. Grid controlled gas tubes were used for combined relays and rectifiers.

The lack of analysis or design procedures for series motor servo systems is an indication of the general mathematically difficult problem of handling non-linear and discontinuous elements. The apparent usefulness of direct current high torque systems warrants an investigation of the response characteristics of series motor systems, and a survey of the difficulty in mathematically describing the motion of the system.

2. Experimental Test System

Relay servomechanism performance is limited by and varies considerably with the parameters of the relay used in the system. A large relay dead zone allows a large position error but lessens the probability of a limit cycle and, conversely, a small dead zone while limiting the position error increases the possibility of a limit cycle. From the foregoing it may be said that increasing the dead zone increases the effective damping of the system since to do so reduces the oscillatory action of the response. An ideal relay would be one with no dead zone whatever, acting precisely in accordance with the applied control signal however small. A system employing an ideal relay would therefore be limited by the characteristics the motor-load combination alone. In the presence of viscous damping the system oscillations would decrease in amplitude and increase in frequency approaching the limit of zero amplitude and infinite frequency. To limit the study to the characteristics of the motor-load combination it was desirable to employ an electronic relay which would very closely approximate an ideal relay rather than use an electromechanical one, thus eliminating the damping effect and position error of a relay with a dead zone.

The system to be tested is shown schematically in Fig. 1 utilizing simple error control of the relay. The relay interrupts the full load current which points out another advantage of the electronic relay, viz., no burning of relay contacts as a result

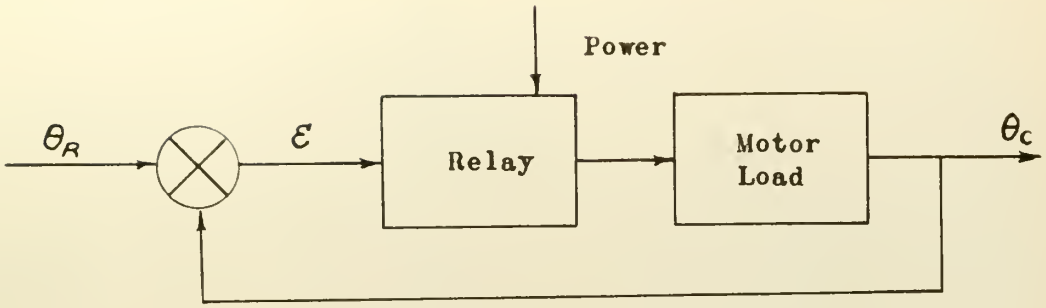

Block Diagram of the Test System
Figure 1

of the repeated switch inherent in relay systems.

The relay consists of two identical gas tube full-wave rectifiers, grid controlled by a square wave generator whose operation is in turn controlled by the error signal. Alternating current power was taken from a 400 cycle 120V generator which when rectified appears to the motor as direct current since an 800 cycle/sec. ripple is well above the motor response capabilities. A schematic diagram of the relay-rectifier is shown in Fig. 2. Thyratron FG-81A gas tubes used for the rectifier are rated to carry twice the maximum requirement of the motor, and have a peak capacity of two amperes, eight times the motor requirement. The use of a tube of such a large relative capacity minimizes any regulation effect the tube might have due to loading. For the same reason overly large transformers were used in the anode circuit. The thyratrons are connected in push-pull, one pair driving each field or direction of the motor. The tubes are fired by a square wave applied

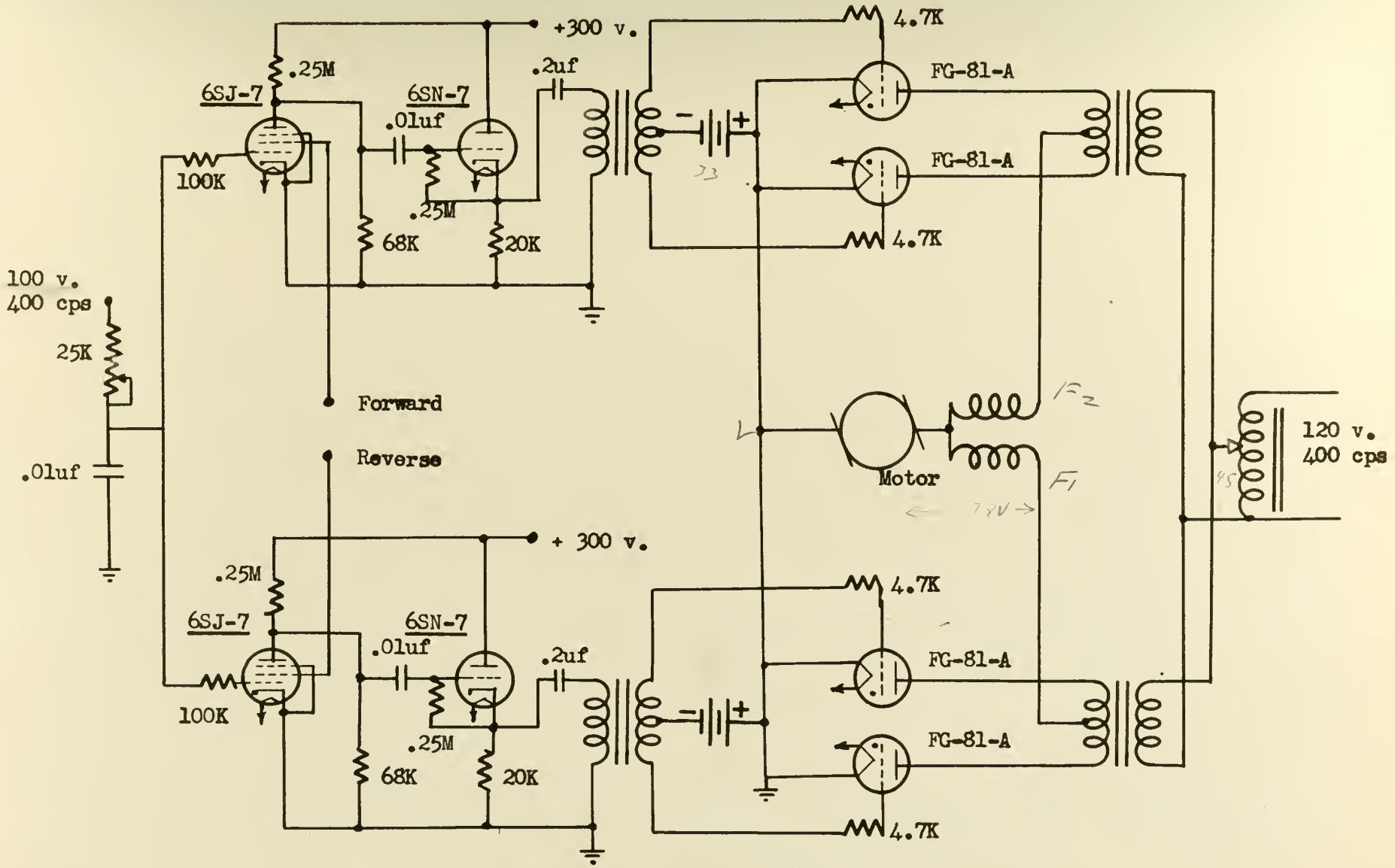

CIRCUIT DIAGRAM OF THE RELAY-RECTIFIER
Figure 2

to the grid transformers, and they extinguish when their respective anode voltages pass through zero potential following removal of the square wave at the grids.

The same line voltage is used to drive the square wave generator which consists of one over-driven pentode amplifier (6SJ-7) and a cathode follower (6SN-7). A phase shifting network was added to exactly match the square wave with the anode voltage thus achieving almost 180^{o} of conduction in each thyratron. A large load resistance was used to limit the current through the pentode then the output voltage was attenuated by shunting the plate to ground through a 68K resistor. The resulting square wave at the thyratron grids is about 35 volts peak to peak. A positive potential at the screen of the pentode determines the existence of the square wave and this level is controlled by the amplified error signal. The gain of the screen grid circuit is such that only a few volts are necessary to cause the square wave to rise to its maximum amplitude.

The system under test was driven by a 1/125 h.p. Electric Indicator Company d.c. split field series motor type FD-37 rated to draw 250 milliamperes at 3600 r.p.m. The split field arrangement allows the motor to be driven by either field, or differentially by both fields. As used herein only one field was energized at a time.

The motor was geared down 244.7 to 1 to provide a system load and to give a substantial sensitivity at the output shaft. A permanent magnet tachometer was added to the system to provide

velocity information and velocity (derivative) feedback to alter the switching times.

An operational amplifier of the Boeing Computer type was used to add and amplify the error and derivative signals. A second amplifier was used as an inverter, and the output of each amplifier controlled the screen grids of the square wave generators in the appropriate rectifier channels. The amplifier connections are shown diagrammatically in Fig. 3 with the appropriate

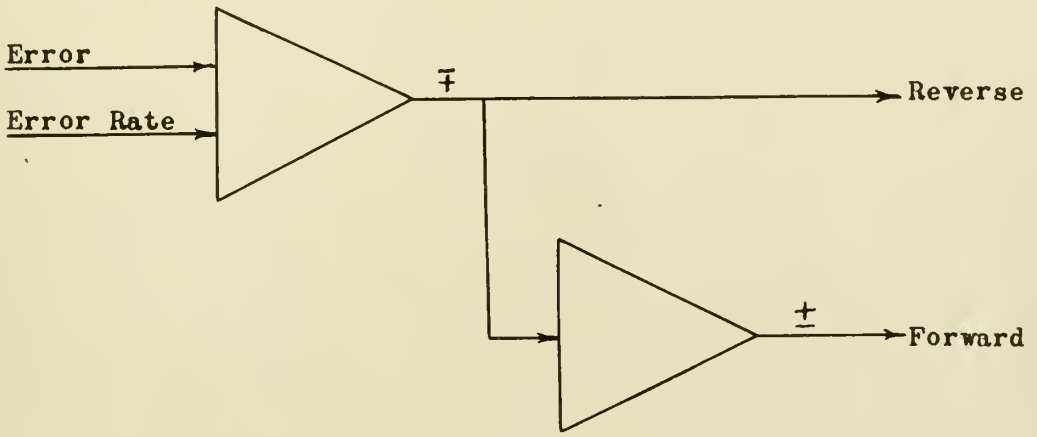

Schematic of Control Amplifier Connections
Figure 3

control polarites indicated. A pseudo-reference signal from a low frequency function generator was added at the first amplifier in voltage form in preference to a mechanical input at the reference control. Error was measured as a voltage between the sliders of two potentiometers in a null-balance fashion; the reference potentiometer remained stationary while the output potentiometer was driven by the output shaft.

The entire test setup is shown in Fig. 4 in schematic form.

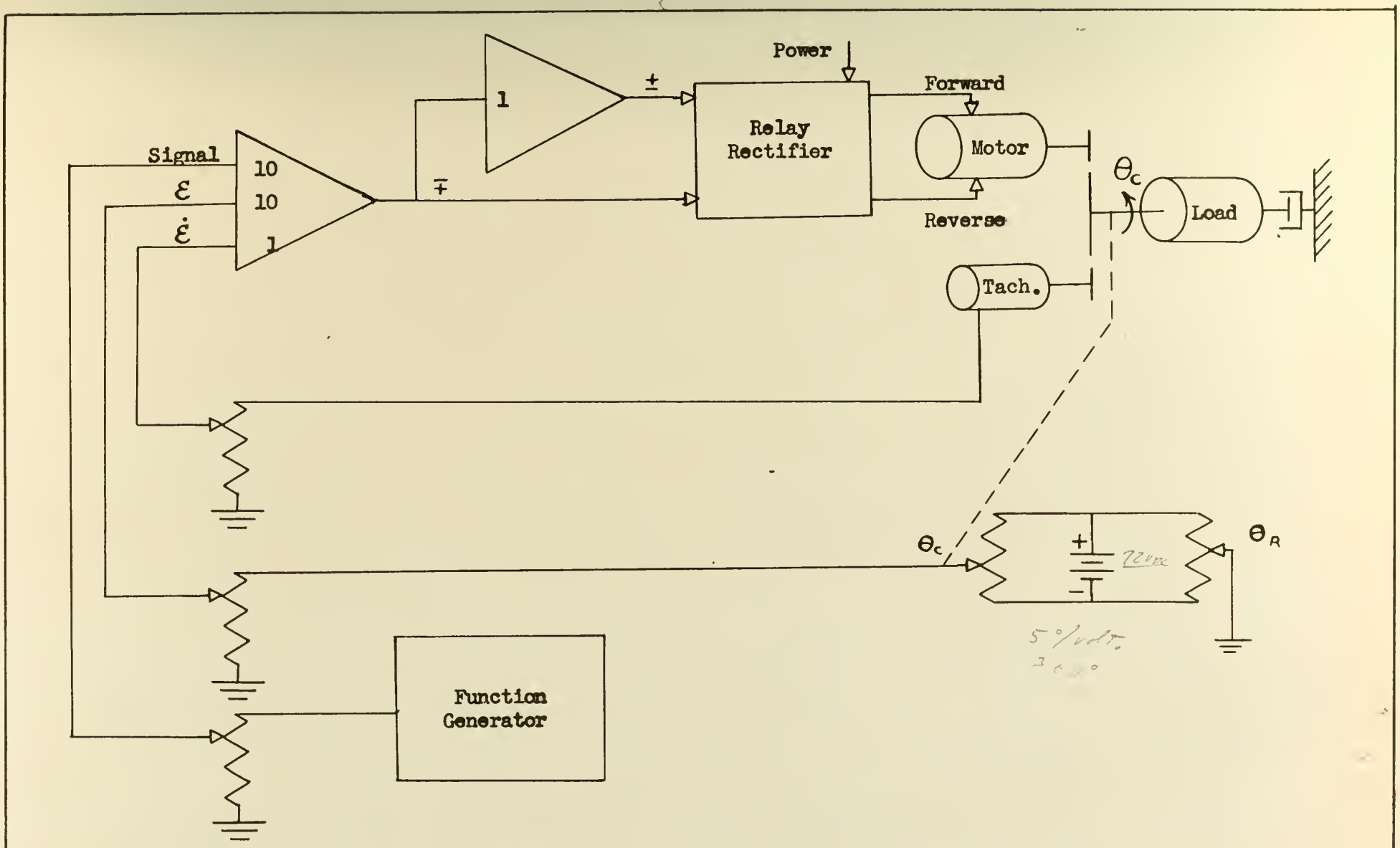

SCHEMATIC DIAGRAM OF THE TEST SET-UP
Figure 4

3. Mathematical Analysis

The split field series motor and a single field series motor may be considered identical electrically for unidirectional control if the inductive effect of a field when cut off may be ignored. With an electromechanical relay the stored energy of the field would be dissipated in the form of a spark discharge at the contacts. Thyratrons acting as relays would only allow discharge during the deionizing period of the gas, but with the field acting as a storage source and the coasting motor acting as a generator the anode potential would be held above that of the cathode allowing almost complete discharge of the stored energy. The gas tube would act as a low impedance and the inductive discharge would be limited by the time constant of the circuit. If the inductive time constant is small with respect to the period of the power frequency, then the inductive effect may be neglected. In this instance, to neglect the inductive effect is justified by experimental results to be shown in a subsequent section. When considering the bidirectional control the second field must be inserted since a reversal of current in the field-armature combination would not reverse the direction of the motor.

Neglecting the drop in the brushes the current in the motor may be expressed by the following differential equation:

$$V = iR + L\frac{di}{dt} + K\phi(RPM) \qquad (1)$$

where R and L includes both the armature and field resistance and inductance. The back e.m.f. of the motor is proportional to the

rate of cutting of flux, i.e., the product of flux and rotational speed. In the linear region of the magnetization curve flux is proportional to armature current and speed is proportional to angular velocity, hence Equation (1) by be re-written as

$$V = iR + L\frac{di}{dt} + K_b i\dot{\theta} \qquad (2)$$

where K_b is the back e.m.f. constant of proportionality. The voltage applied to the system is a constant whose polarity depends upon the sign of the error signal and would always be on in one polarity or the other since with an ideal relay only an infinitesimal control voltage is necessary to shift from one to the other.

Equating the reactive torques to the applied torques of the system shown in Fig. 4 describes the motion of the servo system:

$$J\ddot{\theta} + f\dot{\theta} + C(Sign\,\dot{\theta}) = Ki\phi \qquad (3)$$

and again flux is proportional to armature current and Equation (3) may be written

$$J\ddot{\theta} + f\dot{\theta} + C(Sign\,\dot{\theta}) = K_t i^2 \qquad (4)$$

where K_t is the torque constant.

The simultaneous solution of Equations (2) and (4)

$$V = iR + L\frac{di}{dt} + K_b i\dot{\theta} \qquad (2)$$

$$J\ddot{\theta} + f\dot{\theta} + C(Sign\,\dot{\theta}) = K_t i^2 \qquad (4)$$

is not known in general form, but specific numerical solutions may be obtained in many ways. All methods involve a great deal of labor or the use of analogue or digital computers. An analytic solution would proceed as follows: Differentiating Equation (2)

$$0 = R\frac{di}{dt} + L\frac{d^2i}{dt^2} + K_b\left(\dot{\theta}\frac{di}{dt} + i\dot{\theta}\right) \tag{5}$$

Eliminating $\ddot{\theta}$ between Equations (4) and (5)

$$0 = R\frac{di}{dt} + L\frac{d^2i}{dt^2} + \frac{K_b K_t i^3}{J} - \frac{K_b C i}{J} + K_b\left[\frac{di}{dt} - i\frac{f}{J}\right] \tag{6}$$

Solving Equation (2) for $\dot{\theta}$, substituting in Equation (6) and simplifying

$$L\frac{d^2i}{dt^2} + \frac{di}{dt}\left[\frac{V}{i} + \frac{Lf}{J}i\right] - \frac{L}{i}\left(\frac{di}{dt}\right)^2 + \frac{K_b K_t i^3}{J} - \frac{fV}{J}i + \frac{fR}{J} - \frac{K_b C}{J} = 0 \tag{7}$$

Solution for armature current of Equation (7) is not possible by operational or classical means because of the terms containing second and third degree variables, and products of variables and derivatives. Ordinary linear methods are inadequate in the solution of complex non-linear equations.

A solution may be obtained using an analogue computer in conjunction with two servo or electronic function multipliers. The essentials for a computer solution are shown in Fig. 5, however, there are complicating factors of the problem that are not shown. To express fully the action due to switching power from one field to the other Equations (2) and (4) must be modified.

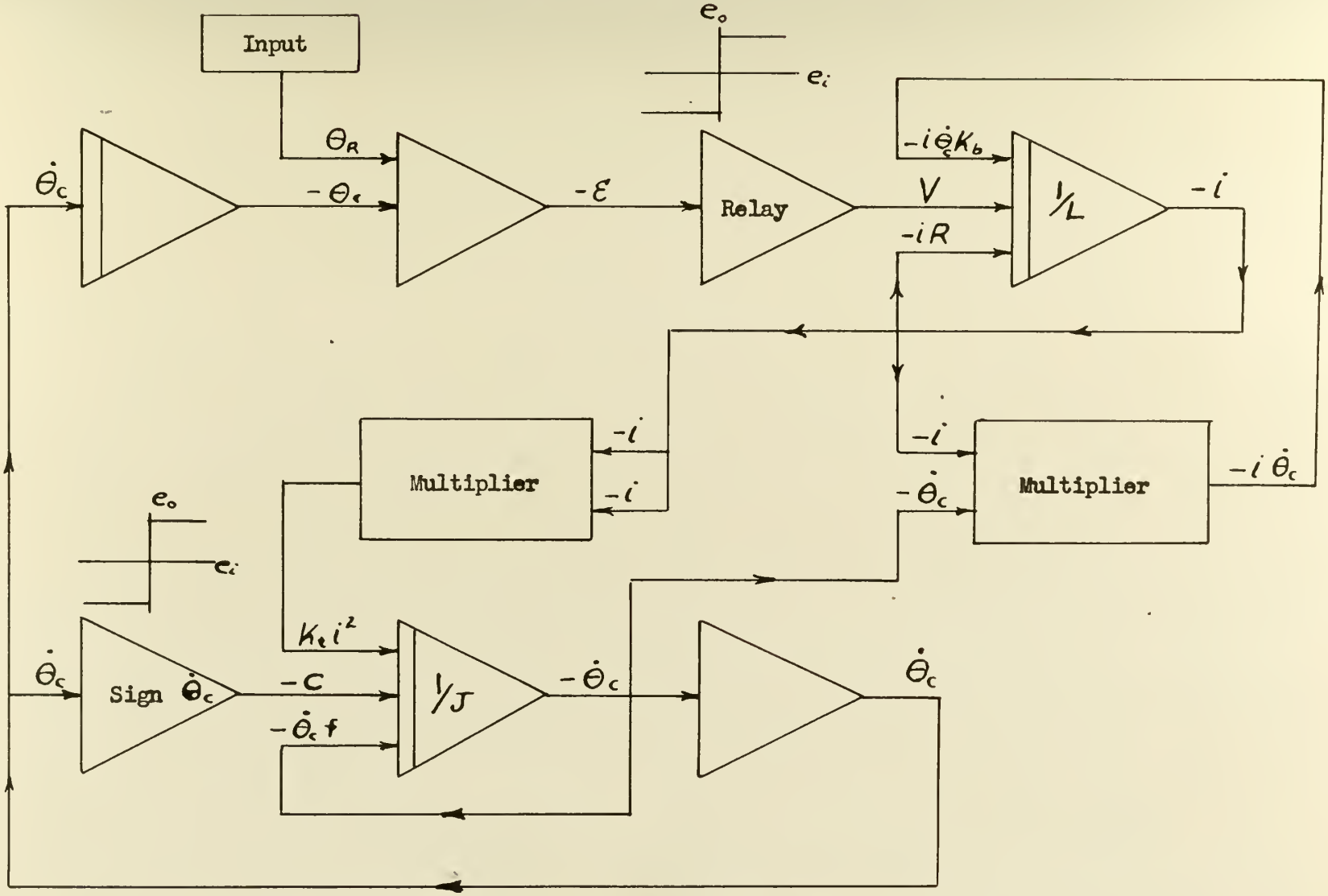

ESSENTIALS OF AN ANALOG COMPUTER SOLUTION
Figure 5

$$V = iR + L\frac{di}{dt} + K_b\, i\,\dot{\theta}\,(Sign\,\mathcal{E}) \qquad (8)$$

$$J\ddot{\theta} + f\dot{\theta} + C\,(Sign\,\dot{\theta}) = K_t\, i^2\,(Sign\,\mathcal{E}) \qquad (9)$$

The above equations assume the use of an ideal relay controlled by the error signal.

The relay simulators are high gain integrating amplifiers whose feed back paths are shunted by diode limiters so that the polarity of the input signal will cause the output to be clamped at a fixed positive or negative level determined by the bias on the feed back limiters (13). One relay simulator is used to act as the ideal relay of the system and another to switch the sign of the coulomb friction input in accordance with the sign of the angular velocity. Additional switching or variation of the circuit is required to account for the reversal of the back e.m.f. and the torque terms in accordance with the polarity of the error signal. This would not be accomplished by the circuit of Fig. 5. In addition the current term must be reduced to zero during switching by shorting the feedback capacitor of the amplifier simulating the motor. This is necessary since, as each field is energized, the current builds up from zero. Upon reversal of the relay the back e.m.f. term becomes a voltage rise rather than a drop allowing a large current to flow until the motor velocity passes through zero and turns in the proper direction for the field that is energized. This large current causes a high reversing

torque since torque is proportional to current squared. A detailed investigation of performance using computer solution is recommended as the subject of another master's thesis.

The describing function technique used to determine performance of many non-linearites can not normally be used for systems containing more than one non-linear element because of the difficulty of handling the product of two describing functions and in many problems the technique would not be valid because of lack of filtering between the non-linear elements. The possibility exists that a single describing function might be written for two elements in cascade but in the problem at hand such a describing function would require the analytical solution of the equations which is not available, and the remainder of the servo system would not provide any filtering of the output harmonics whatever. For the above reasons the describing function technique as developed today can not be used in this problem.

The non-linear mechanics technique of phase-plane analysis can be used although the method would require laborious crossplotting between an error phase-plane, and the armature current phase-plane. To account for the change of field and reversal of coulomb friction with direction of rotation Equations (4) must be modified as follows:

$$J\ddot{\theta} + f\dot{\theta} + C\,(sign\,\dot{\theta}) = K_t i^2\,(-sign\,\mathcal{E}) \tag{10}$$

Substituting variables to express the equations in terms of error

$$V = iR + L\frac{di}{dt} - K_b i\dot{\mathcal{E}} \tag{11}$$

$$J\ddot{\mathcal{E}} + f\dot{\mathcal{E}} + C(\text{sign}\,\dot{\mathcal{E}}) = K_t i^2 (\text{sign}\,\mathcal{E}) \tag{12}$$

Equation (12) may be rearranged

$$\ddot{\mathcal{E}} = -\left[\frac{f}{J}\dot{\mathcal{E}} + \frac{C}{J}(\text{sign}\,\dot{\mathcal{E}}) - \frac{K_t}{J} i^2 (\text{sign}\,\mathcal{E})\right] \tag{13}$$

Dividing by error rate

$$\frac{\ddot{\mathcal{E}}}{\dot{\mathcal{E}}} = \frac{d\dot{\mathcal{E}}}{d\mathcal{E}} = -\frac{\left[\frac{f}{J}\dot{\mathcal{E}} + \frac{C}{J}(\text{sign}\,\dot{\mathcal{E}}) - \frac{K_t}{J} i^2 (\text{sign}\,\mathcal{E})\right]}{\dot{\mathcal{E}}} \tag{14}$$

Equation (14) is in the general form required for plotting a phase-plane by the delta method where the term in the brackets is measured positive to the left from the origin along the horizontal error axis. In a similar manner Equation (11) may be put into the delta form:

$$\frac{di}{dt} = -\left[i\frac{R}{L} - \frac{V}{L} - \frac{K_b}{L} i\dot{\mathcal{E}}\right] \tag{15}$$

Differentiating Equation (15)

$$\frac{d^2 i}{dt^2} = -\left[\frac{di}{dt}\frac{R}{L} - \frac{K_b}{L}\left(i\ddot{\mathcal{E}} + \dot{\mathcal{E}}\frac{di}{dt}\right)\right] \tag{16}$$

Substituting for $\ddot{\mathcal{E}}$ from Equation (13)

$$\frac{d^2 i}{dt^2} = -\left[\frac{K_b}{L} i\left(\frac{f}{J}\dot{\mathcal{E}} + \frac{C}{J}\text{Sign}\,\dot{\mathcal{E}} - \frac{K_t}{J} i^2 \text{Sign}\,\mathcal{E} + \frac{di}{dt}\left(\frac{R}{L} - \frac{K_b}{L}\dot{\mathcal{E}}\right)\right]\right] \tag{17}$$

$$\frac{d^2 i}{dt^2} \Big/ \frac{di}{dt} = -\frac{\left[\frac{K_b}{L} i\left(\frac{f}{J}\dot{\mathcal{E}} + \frac{C}{J}\text{Sign}\,\dot{\mathcal{E}} - \frac{K_t}{J} i^2 \text{Sign}\,\mathcal{E} + \frac{di}{dt}\left(\frac{R}{L} - \frac{K_b}{L}\dot{\mathcal{E}}\right)\right]\right]}{\frac{di}{dt}} \tag{18}$$

Equation (18) is in the delta form but the difficulty of using this equation to plot a phase-plane is obvious. The two phase-planes must be plotted simultaneously since the determination of each delta term requires end point information because each contains a variable of the other plot. The method requires an initial estimate of one variable to determine the second variable which can then be used to revise the initial estimate, and the procedure iterated for each point of the plots until agreement is reached.

As an alternative to the two phase-plane method Equation (15) may be solved as a transient and the position phase plane coordinated through the time variable. This requires considerable iteration between the two plots as in the first method.

Only one phase-plane trajectory need be plotted for the initial phase since the trajectory would be identical for all magnitudes of step input and a template could be used to draw in any other trajectories desired. The trajectories after switching are similar but initially depend upon the error rate at switching hence the use of a template would be more complicated but still practical.

From the foregoing it becomes obvious why no mathematical analysis of the series motor has been published, continued study is warranted since the motor possesses characteristics that are extremely valuable in a relay system as will be shown.

4. Determination of System Parameters

The motor was mounted in a special dynamometer that measures shaft torque. Torque-speed data was taken using both fields driven by direct current and pulsed d.c. from the rectifier unit. For practical purposes the fields were found to be identical (within 2%) and runs made with different power supplies were indistinguishable from one another. The torque-speed curves of the motor are shown in Fig. 6 and although their slope does not vary as much as 10 to 1 there is a significant difference from low to high speed. It will be assumed that linearization is not possible here since other series motors show a more pronounced curvature. Some variation of the curves with temperature was noted therefore the motor was run for 30 minutes prior to all data runs.

A plot of torque as the square of armature current verifies the assumption that flux varies directly with current in a considerable region of the magnetization curve. Fig. 7 shows the linearity of this relation with no deviation below 180m.a. increasing to 12.5% variation at full load current. The torque intercept is the torque that must be overcome before useful output torque can be realized, hence it is the torque due to coulomb friction (C_{motor} = 4.25 oz-in). The current intercept is the current required to just balance the drag of coulomb friction (i = 70m.a.). The slope of the linear line is taken to be the torque constant of the motor (K_t = 8.5 x 10^{-4} oz-in/m.a.^{2}). Coulomb friction of the motor calculated using the torque constant and the current intercept is:

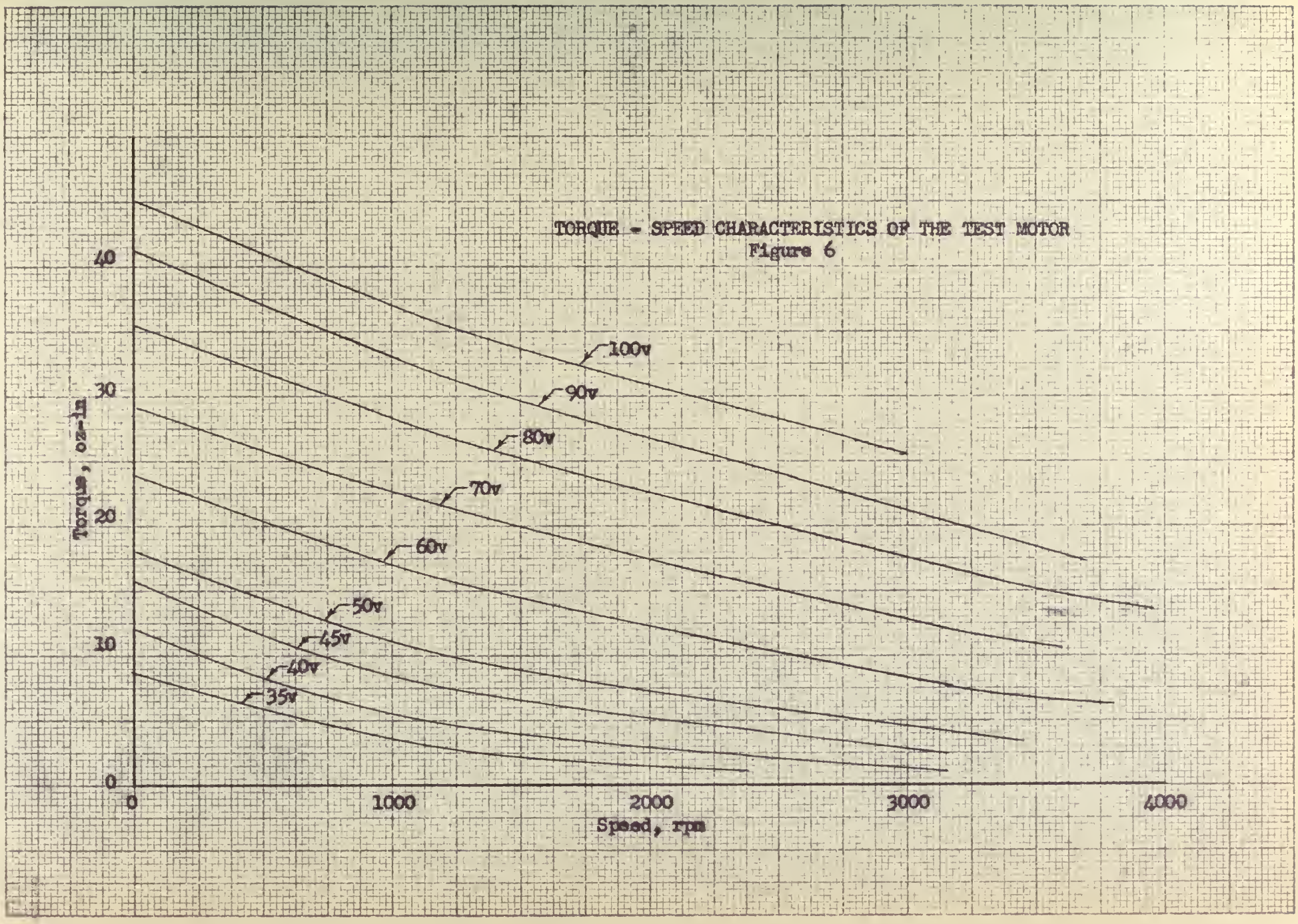
TORQUE - SPEED CHARACTERISTICS OF THE TEST MOTOR
Figure 6
Torque, oz-in
40
30
20
10
0
100v
90v
80v
70v
60v
50v
45v
40v
35v
0
1000
2000
3000
4000
Speed, rpm

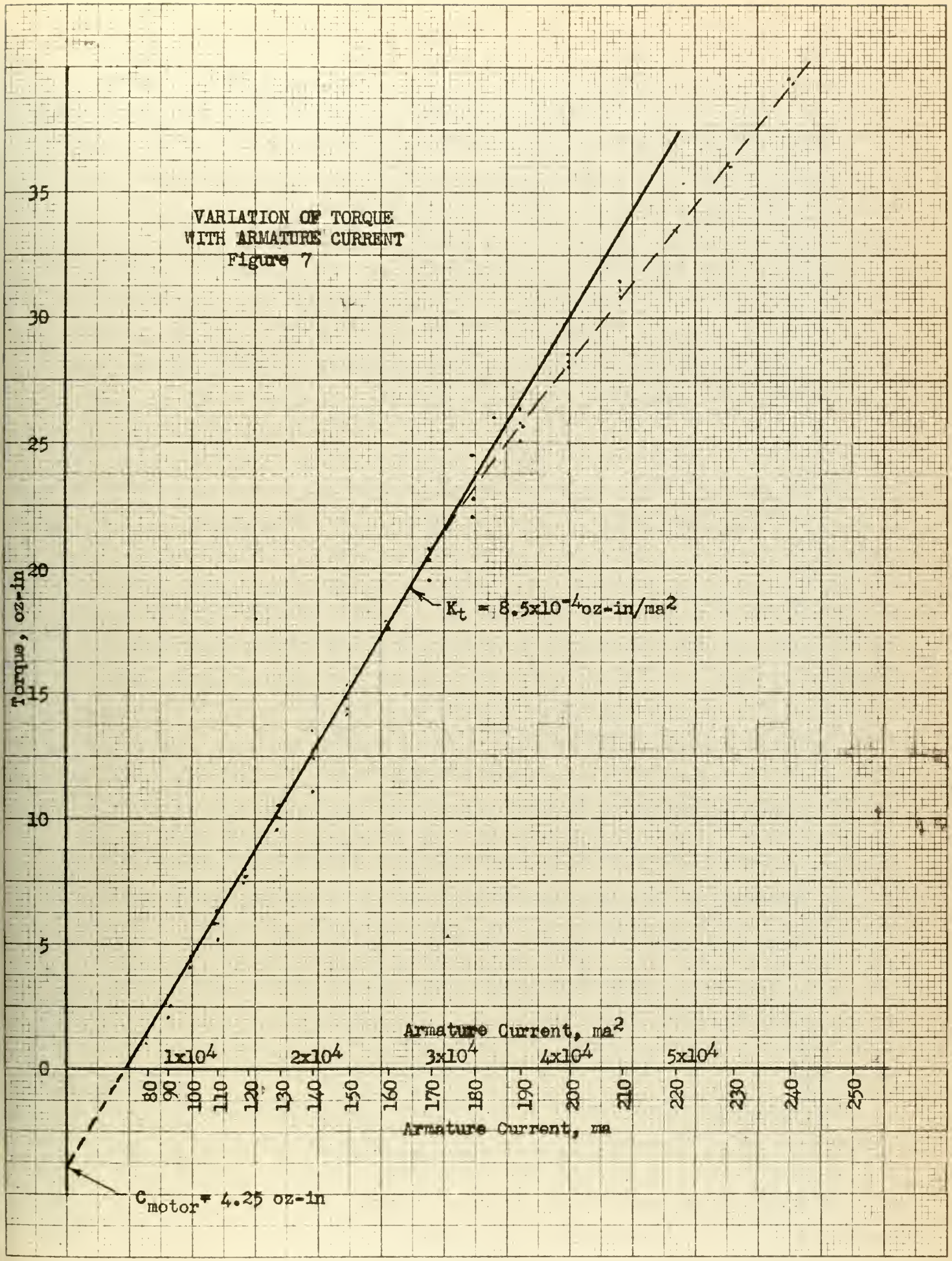
VARIATION OF TORQUE
WITH ARMATURE CURRENT
Figure 7
Torque, oz-in
35
30
25
20
15
10
5
0
$K_t = 8.5 \times 10^{-4}$ oz-in/ma^2
Armature Current, ma^2
1x10^4
2x10^4
3x10^4
4x10^4
5x10^4
80
90
100
110
120
130
140
150
160
170
180
190
200
210
220
230
240
250
Armature Current, ma
C_{motor} = 4.25 oz-in

$$C_{motor} = 8.5 \times 10^{-4} \times 70^2 = 4.17 \text{ oz-in}$$

The stall torque of the motor is plotted in Fig. 8; the voltage intercept (20v) corresponds to the current intercept of Fig. 7 and the resistance obtained from these two values equals the armature resistance measured by an ohmeter (R = 285 ohm).

$$R = \frac{20}{.07} = 285.7 \text{ ohm}$$

This verifies the value of coulomb friction already found since Equation (2) and (4) degenerate at stall to the following:

$$V = i R \tag{19}$$

$$C = K_t i^2 \tag{20}$$

The inductance of the motors field and armature combined were measured using a General Radio Impedance Bridge at 1000 cps, these values were found to be

$$L_1 = .40 \text{ heneries}$$

$$L_2 = .30 \text{ heneries}$$

With the motor assembled in the gear train the total inertia was determined using the deceleration test with added inertia disks (14). Deceleration time to 50% speed was used as standard on all runs plotted in Fig. 9 and the negative inertia intercept is the total inertia of the motor-load combination.

$$J = .6 \text{ oz-in}^2$$

The tachometer output was calibrated by timing ten revolutions of the output shaft. The calibration is shown in Fig. 10 where the slope of the curve is the tachometer voltage constant:

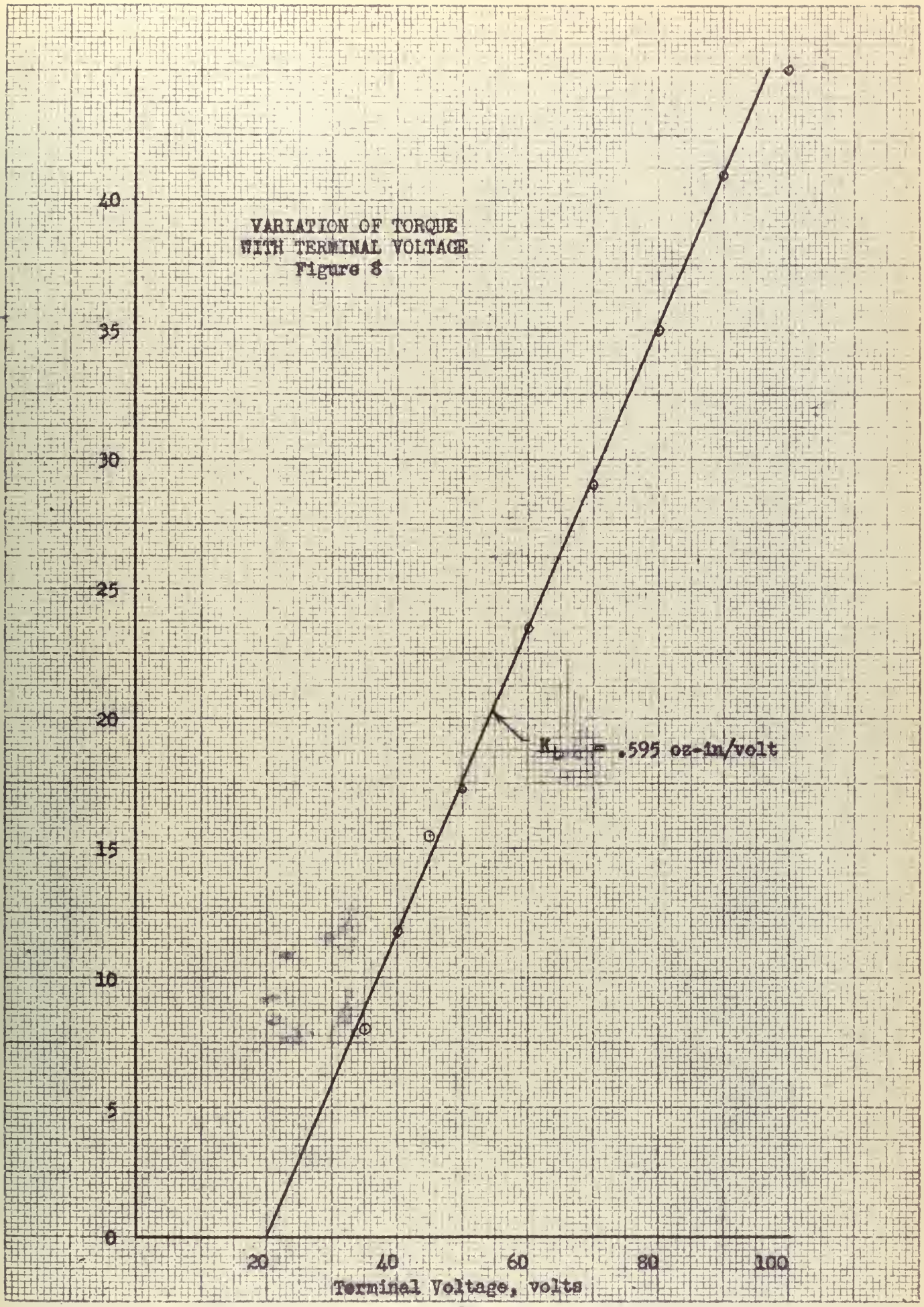
VARIATION OF TORQUE
WITH TERMINAL VOLTAGE
Figure 8
$K_{b_{n-l}}$ = .595 oz-in/volt
40
35
30
25
20
15
10
5
0
20
40
60
80
100
Terminal Voltage, volts

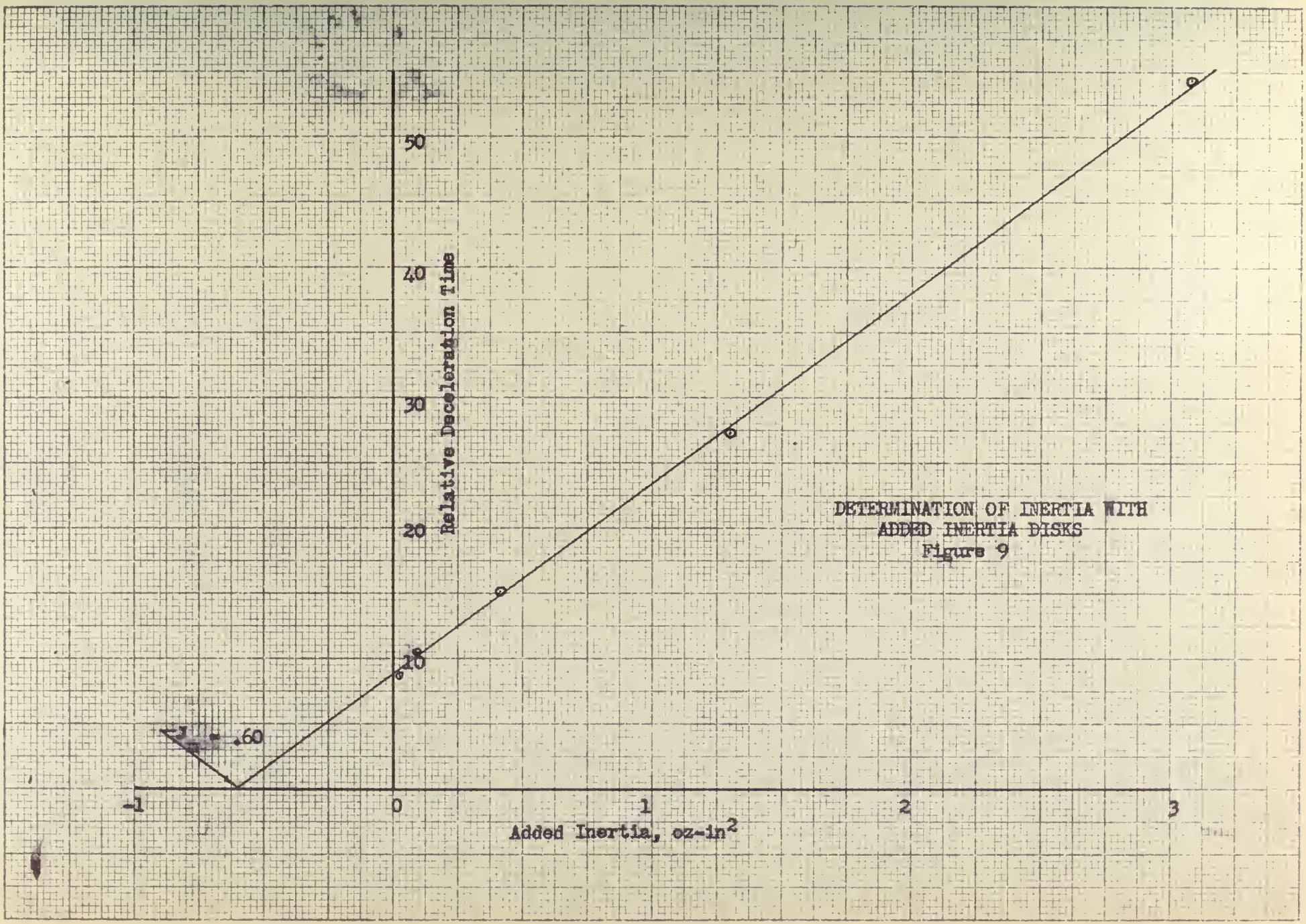

DETERMINATION OF INERTIA WITH
ADDED INERTIA DISKS
Figure 9

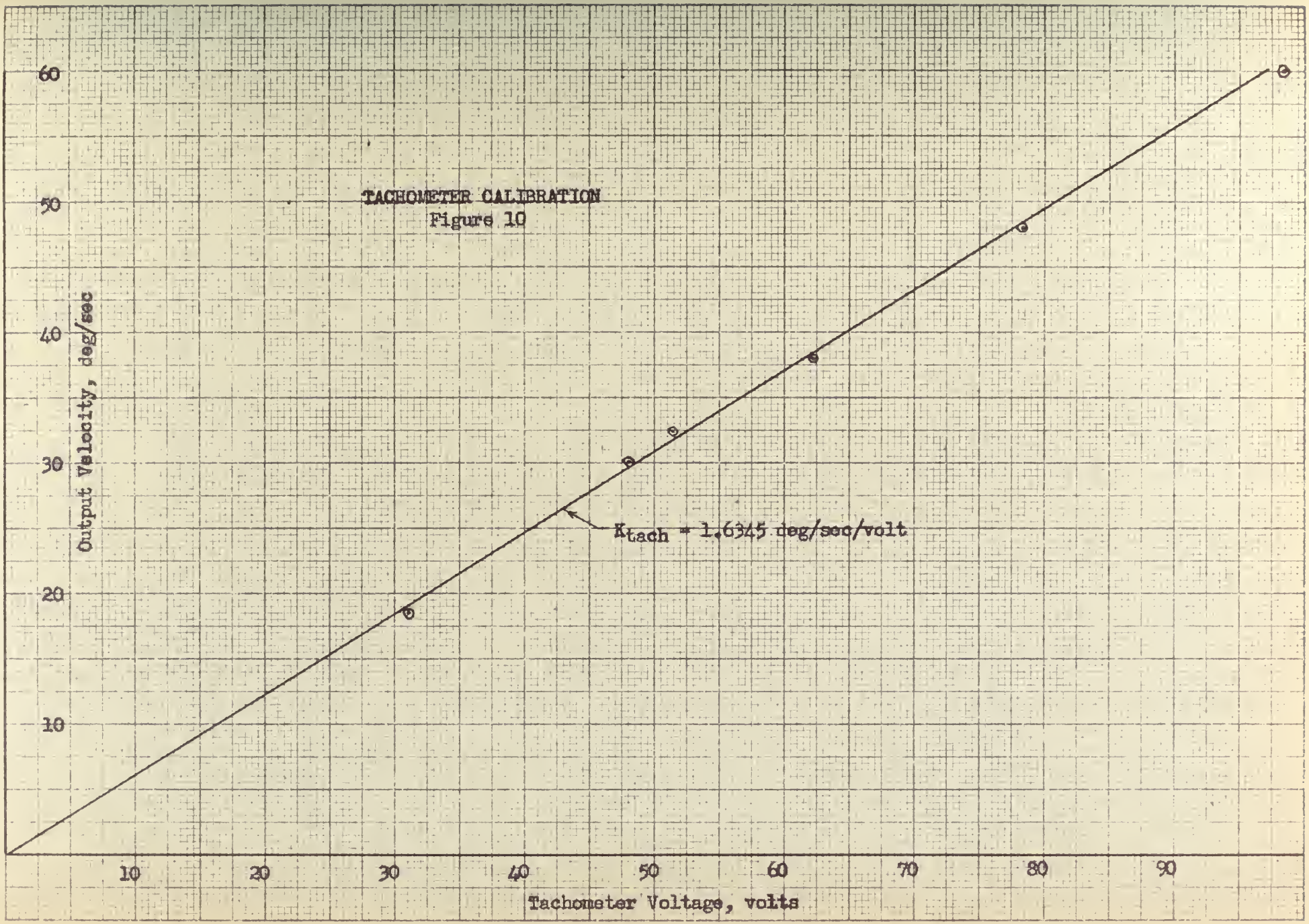
TACHOMETER CALIBRATION
Figure 10
Output Velocity, deg/sec
60
50
40
30
20
10
K_{tach} = 1.6345 deg/sec/volt
10
20
30
40
50
60
70
80
90
Tachometer Voltage, volts

K_{tach} = 1.6345 degrees/sec/volt.

Coulomb and viscous friction were determined by steady state testing; Equation (4) becomes

$$f\dot{\theta} + C = K_t i^2 \tag{21}$$

Current and velocity were determined at several steady state speeds and were plotted in Fig. 11 indicating the friction components to have the values:

C_m = 9.1 oz-in

F_m = 7.29 x 10^{-5} oz-in/degree/sec

It is noted that at rated speed viscous friction accounts for only 16% of the frictional drag, the remainder being due to coulomb friction.

The back e.m.f. constant of the motor was found by steady state testing measuring voltage, current and velocity. Equation (2) in steady state degenerates to:

$$V = iR + K_b i\dot{\theta} \tag{22}$$

The back e.m.f. constant was determined to be

K_b = 1.1 volts/m.a./degree/sec

All the parameters thus far have been determined in terms of the motor shaft, to be useful these must be converted through the gear ratio to the output shaft. Table I lists all the system parameters referred to both the motor and output shaft.

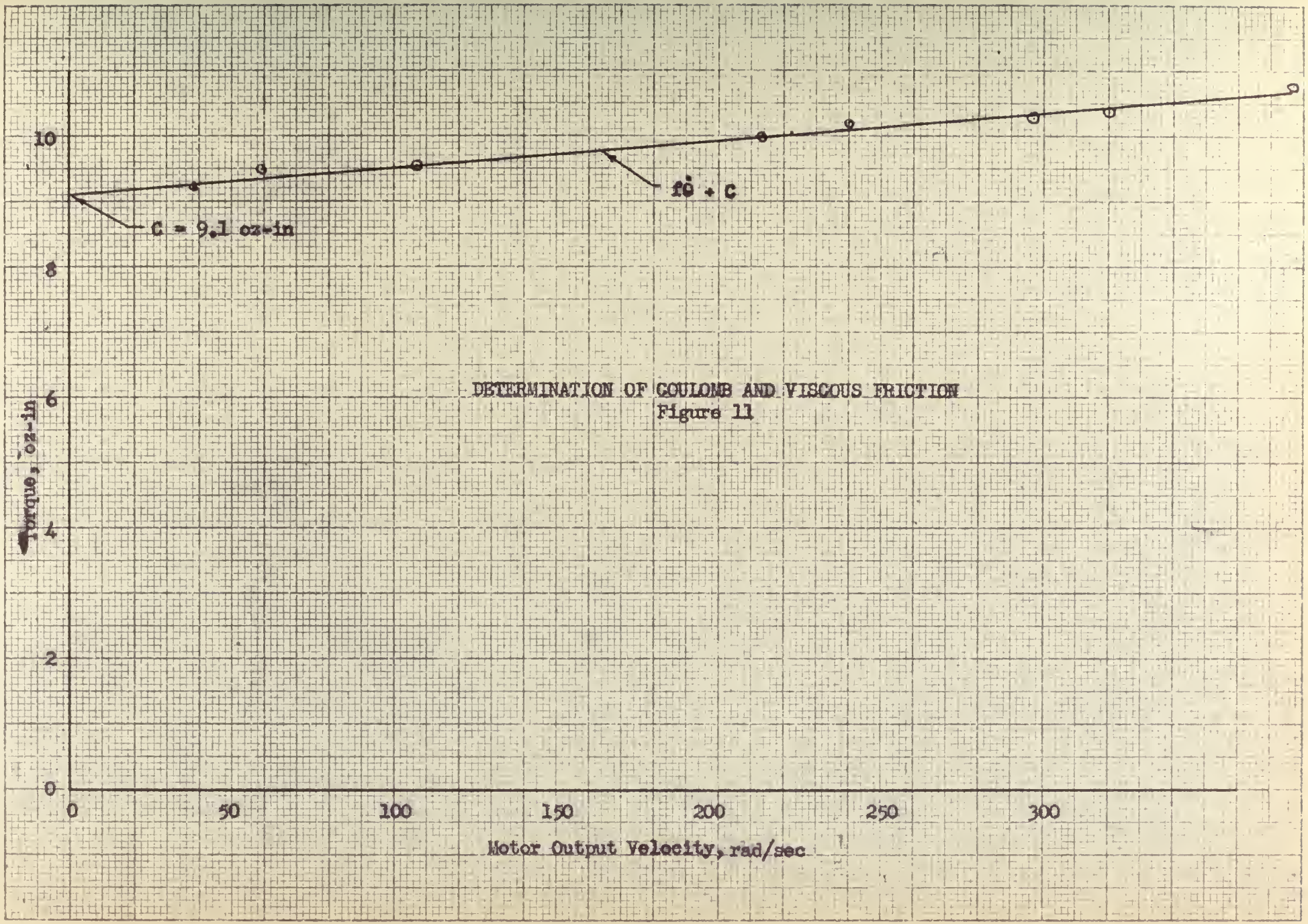

DETERMINATION OF COULOMB AND VISCOUS FRICTION
Figure 11

TABLE I

SYSTEM PARAMETERS

PARAMETER		UNIT	MOTOR	OUTPUT
MOTOR:				
Resistance	R	ohms	285	285
Inductance	L	heneries	.3 - .4	.3 - .4
Coulomb Friction	C	oz-in	4.17	1020.4
Torque Constant	K_t	oz-in/ma^2	$.85 \times 10^{-3}$	.208
SERVO SYSTEM:				
Inertia	J	oz-in^2	.60	146.82
Viscous Friction	F	oz-in/deg/sec	1.1×10^{-4}	.026917
Coulomb Friction	C	oz-in	9.1	2226.8
Bach e.m.f. Constant	K_b	V/ma/deg/sec	1.1	269.2
Tachometer Constant	K_{tach}	V/deg/sec	1.6345	399.96
Gear Ratio			244.7	1
Motor Voltage	V	Volts	78	

The relay characteristic of the rectifier unit was determined to be as shown in Fig. 12; the relay has a dead zone that can be reduced to one quarter of a degree without spurious firing of the thyratrons occurring. With the minimum dead zone full current is available outside of 2.25° from the zero position. This relay, although not ideal in that a dead zone is present and its switching lines are not vertical, does act much more as an ideal one than does any electromechanical relay. The sensitivity could be increased by increasing the voltage across the error measuring potentiometers above the .2v/degree that was used.

SWITCHING CHARACTERISTICS OF THE RELAY-RECTIFIER
Figure 12

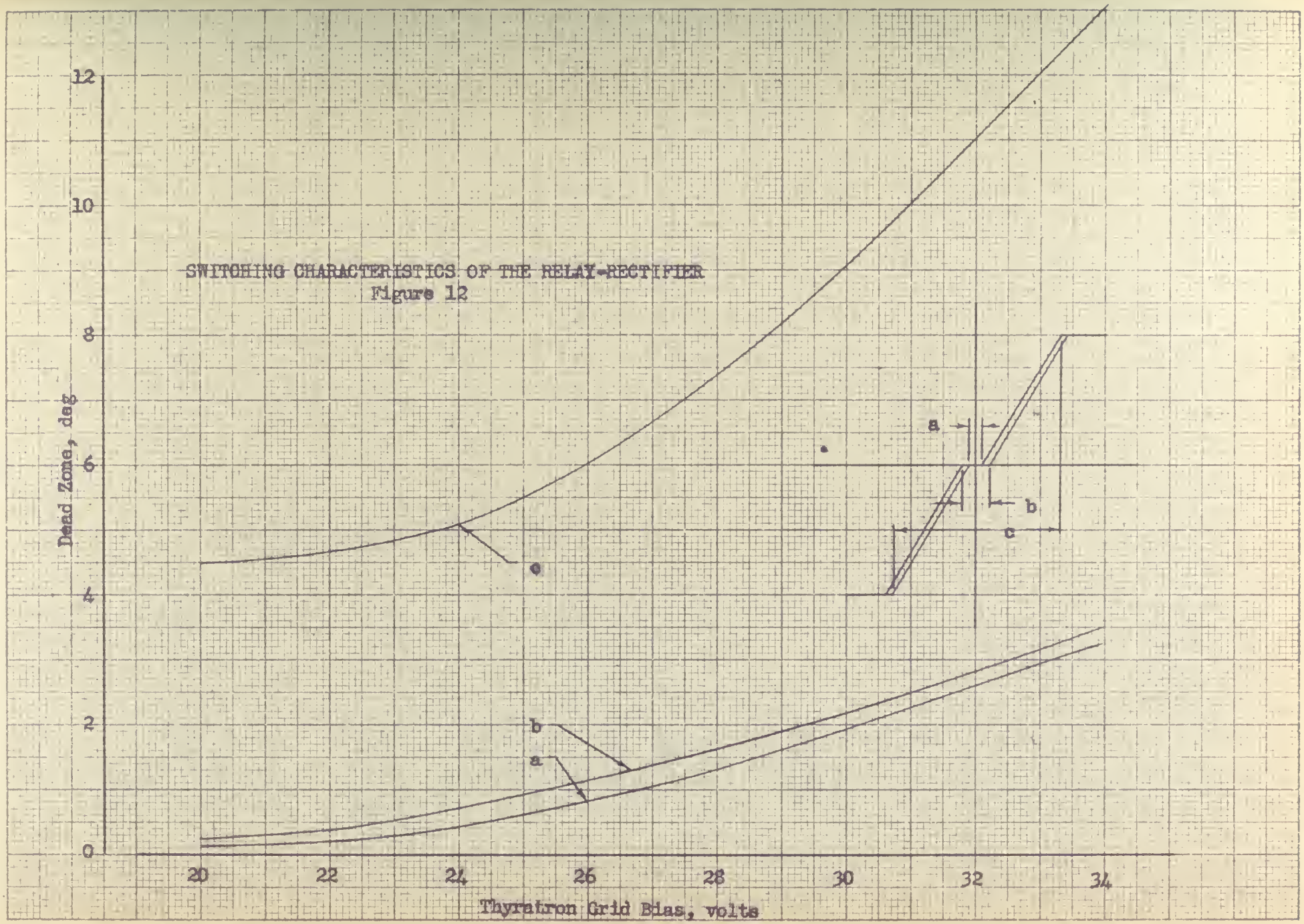

5. System Response to Error Control

The relay was adjusted to give a minimum dead zone of one quarter of a degree by setting the thyratron bias level at 22.5 volts; this setting remained constant except as indicated. The spread of the dead zone at full current is 4.75 degrees which is in itself a small dead zone. The sloping character of the relay characteristic lines allows a small variation from full response near the switching points but does not greatly affect overall response.

The system was tested for transient response with step inputs of several different amplitudes approaching velocity saturation. The response to step imputs are shown in Fig. 13. It is noted that there is no indication of limit cycle operation as might be expected of a relay servo employing an ideal relay. In each instance the system pulled into the dead zone despite its narrowness in less than two cycles of oscillation. Rise time, delay time and settling-out time are all direct functions of step amplitude and are not true performance criteria for relay systems. The variation of peak overshoot with step amplitude is shown in Fig. 14 to be a decreasing function as might be expected since magnitude of deceleration current following switching is a function of angular velocity, hence magnitude of step input.

The phase-plane plot of the transient data in Fig. 15 shows quite clearly the validity of using the response to a large step as a pattern for all smaller step inputs in that the largest trajectory might be moved horizontally to any starting position and

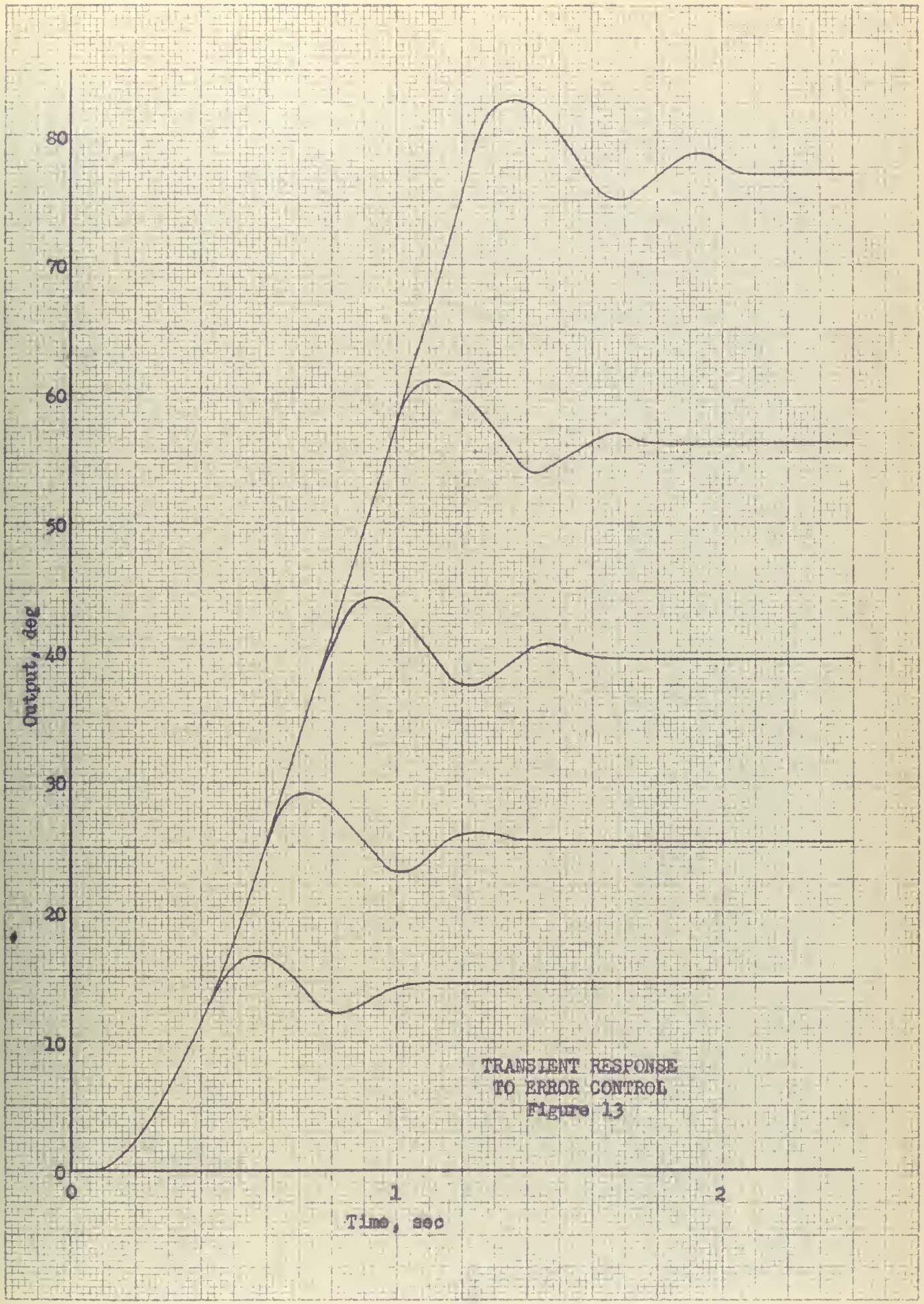

TRANSIENT RESPONSE
TO ERROR CONTROL
Figure 13

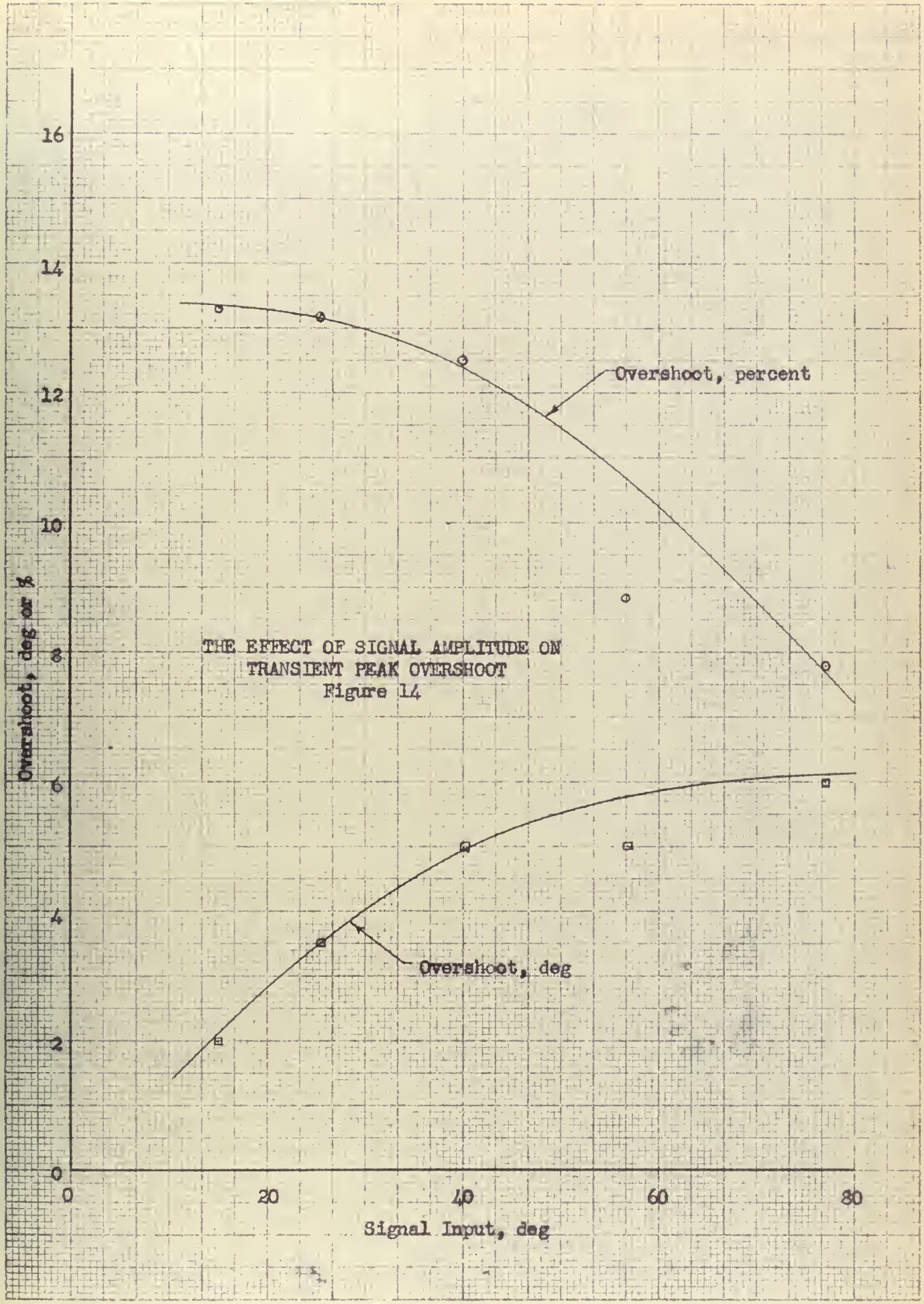

THE EFFECT OF SIGNAL AMPLITUDE ON
TRANSIENT PEAK OVERSHOOT
Figure 14

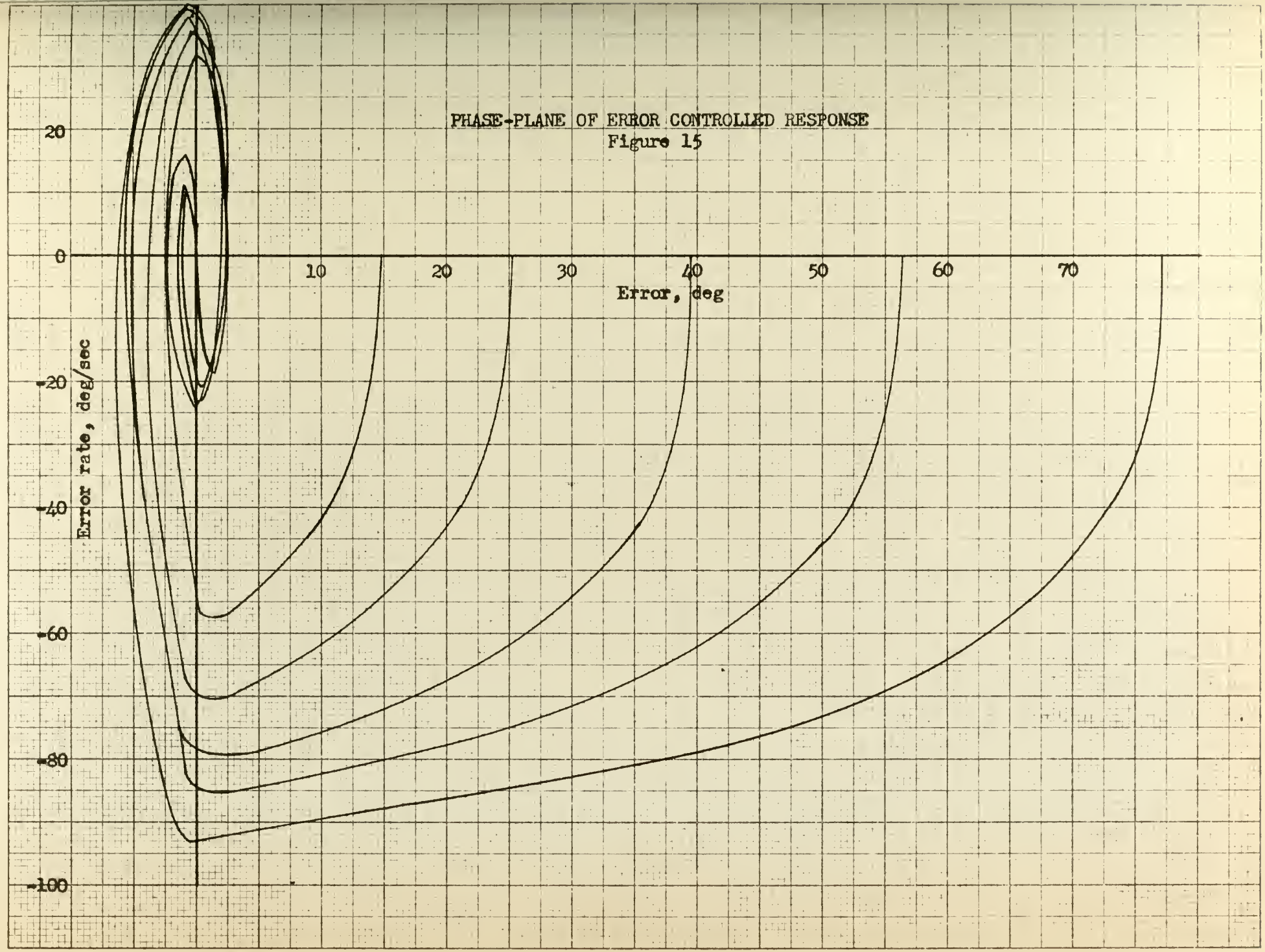

PHASE-PLANE OF ERROR CONTROLLED RESPONSE
Figure 15

the trajectory up to switching traced out. The super-deceleration due to the current surge at switching is apparent at the switching lines where the trajectories are nearly vertical. The effect of the sloping relay characteristic can be seen as the trajectories droop as they approach switching and immediately following switching. With straight side relay characteristics the deceleration would be even more pronounced.

The system was tested for frequency response using signal amplitudes up to a peak value equal to the largest step input that was used. Three typical response curves are shown in Fig. 16. In general the lag angle increases suddenly at about the resonant frequency, with the sharper break at lower signals resulting in higher resonant peaks. The sharp break of lag angle is a common characteristic of non-linear devices.

The frequency response was converted to open loop response by using the Nichols M-N Contour Chart as shown in Fig. 17. These plots are limited in that small lag angles are difficult to plot. For small signal runs only that portion of the frequency response above the resonant peak can be shown. This limits the presentation of the Bode Diagrams of Fig. 18. For the values shown the initial slope varies from -30db/octave to -54 db/octave breaking sharply to -12db/octave near the resonant frequency. The phase angle appears to rise sharply from -180° to about -120°, hook at the resonant frequency then round off toward -180° for the higher frequencies. The phase margin varies between 45° and 60° for all amplitudes of input sine waves indicating the reason for the

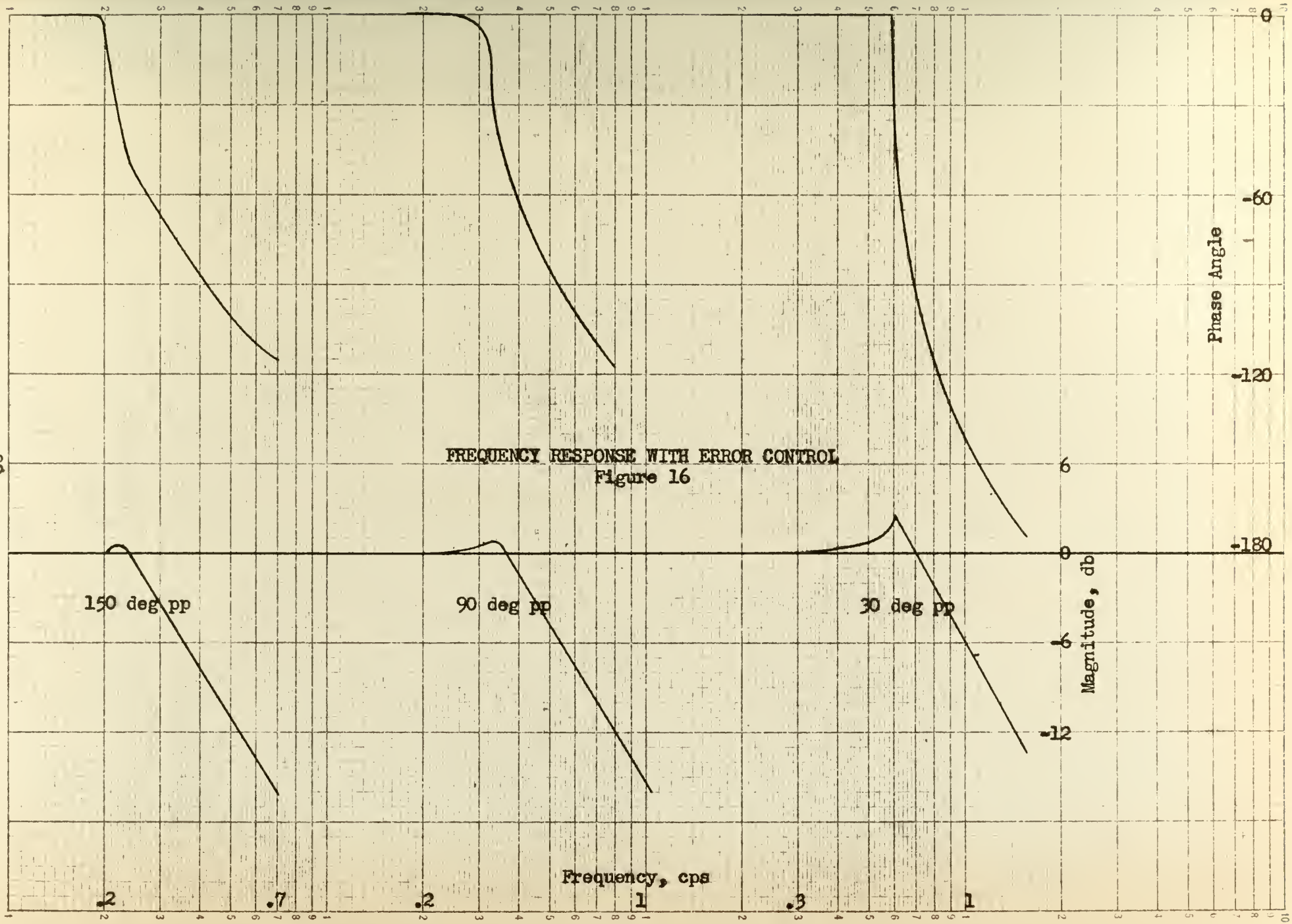

FREQUENCY RESPONSE WITH ERROR CONTROL
Figure 16

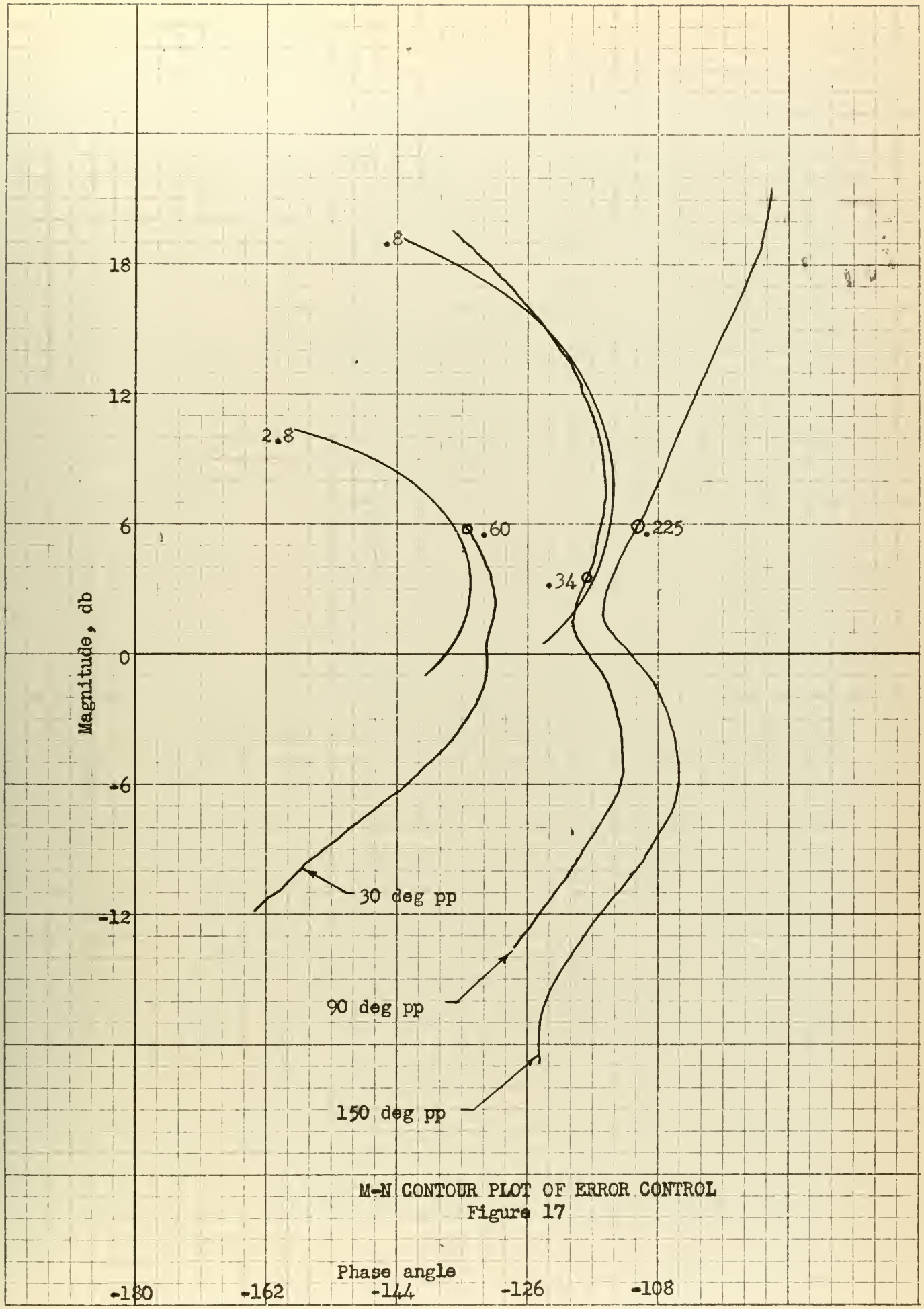

M-N CONTOUR PLOT OF ERROR CONTROL
Figure 17

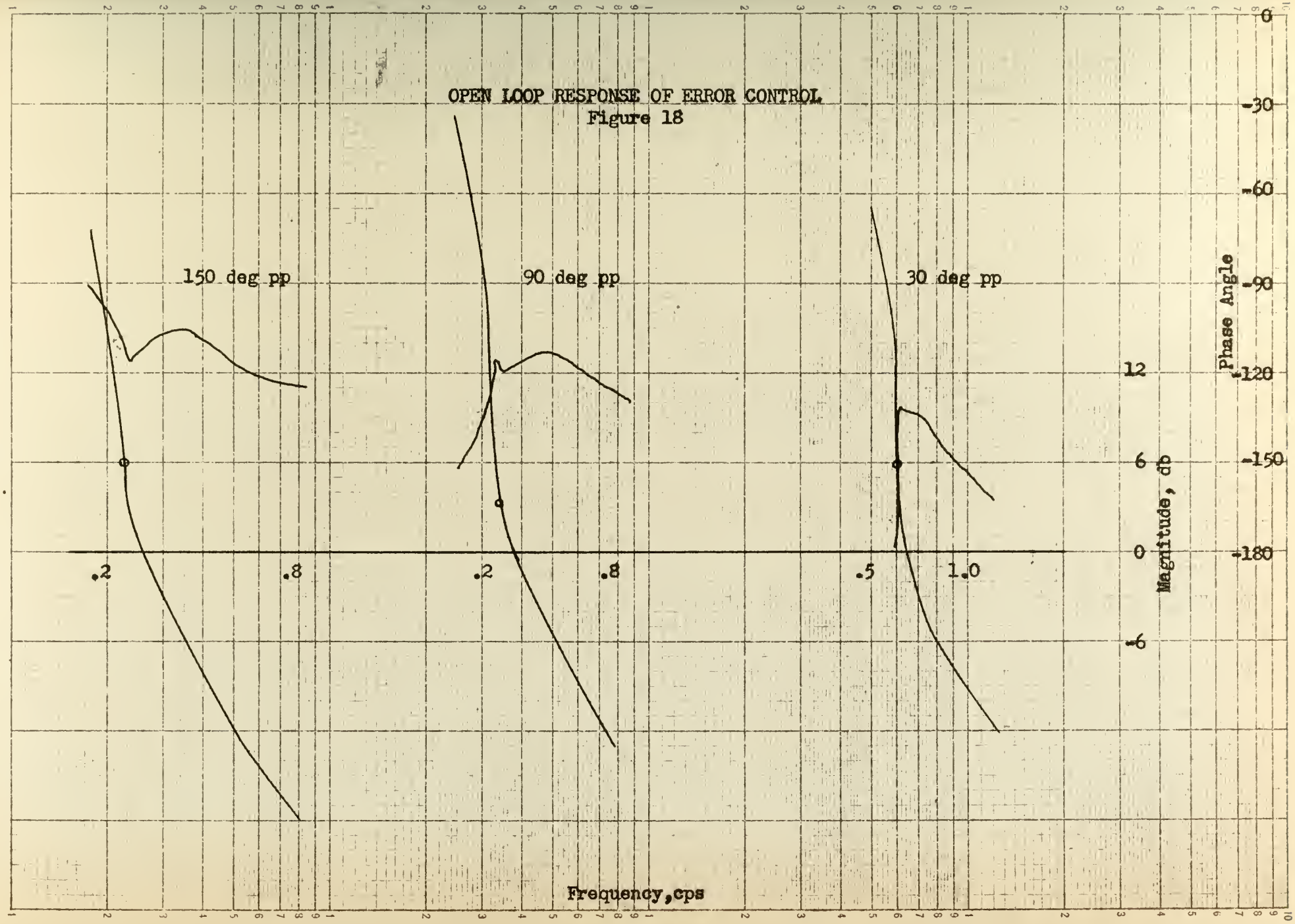
OPEN LOOP RESPONSE OF ERROR CONTROL
Figure 18
150 deg pp
90 deg pp
30 deg pp
.2
.8
.2
.8
.5
1.0
12
6
0
-6
0
-30
-60
-90
-120
-150
-180
Phase Angle
Magnitude, db
Frequency, cps

absence of a limit cycle. The plots would suggest a "Type 2" system of about eighth order if this were a linear system, but with "variable" time constants.

Such a transfer function is beyond the present state of the art and will not be considered further. The information in the Bode Diagram of Fig. 18 was converted to a Nyquist plot in Fig. 19. The plots are quite similar in shape in the low magnitude regions with the phase margin increasing slightly with signal amplitude. Although the frequency of resonance decreases with increasing signal it is noted that the points corresponding to resonance are on or near the circle of open loop gain ratio = 2. The low frequency end of the curve for the maximum signal is believed to be in error due to the difficulty of measuring very small frequency response phase angles when the output wave is stepping due to relay action. All curves should approach -180° at low frequencies for a "Type 2" system.

The variation of resonant frequency and resonant magnitude with signal amplitude is shown in Fig. 20 in a variety of cross plots. These plots although continuous are non-linear relations with one exception. Magnitude ratio in decibels appears to be an inverse logarithmic function of signal amplitude, i.e.,

$$\text{Log } M = \frac{A}{\text{Log } \theta_c} \tag{23}$$

or

$$\text{Log } M \text{ Log } \theta_c = A \tag{24}$$

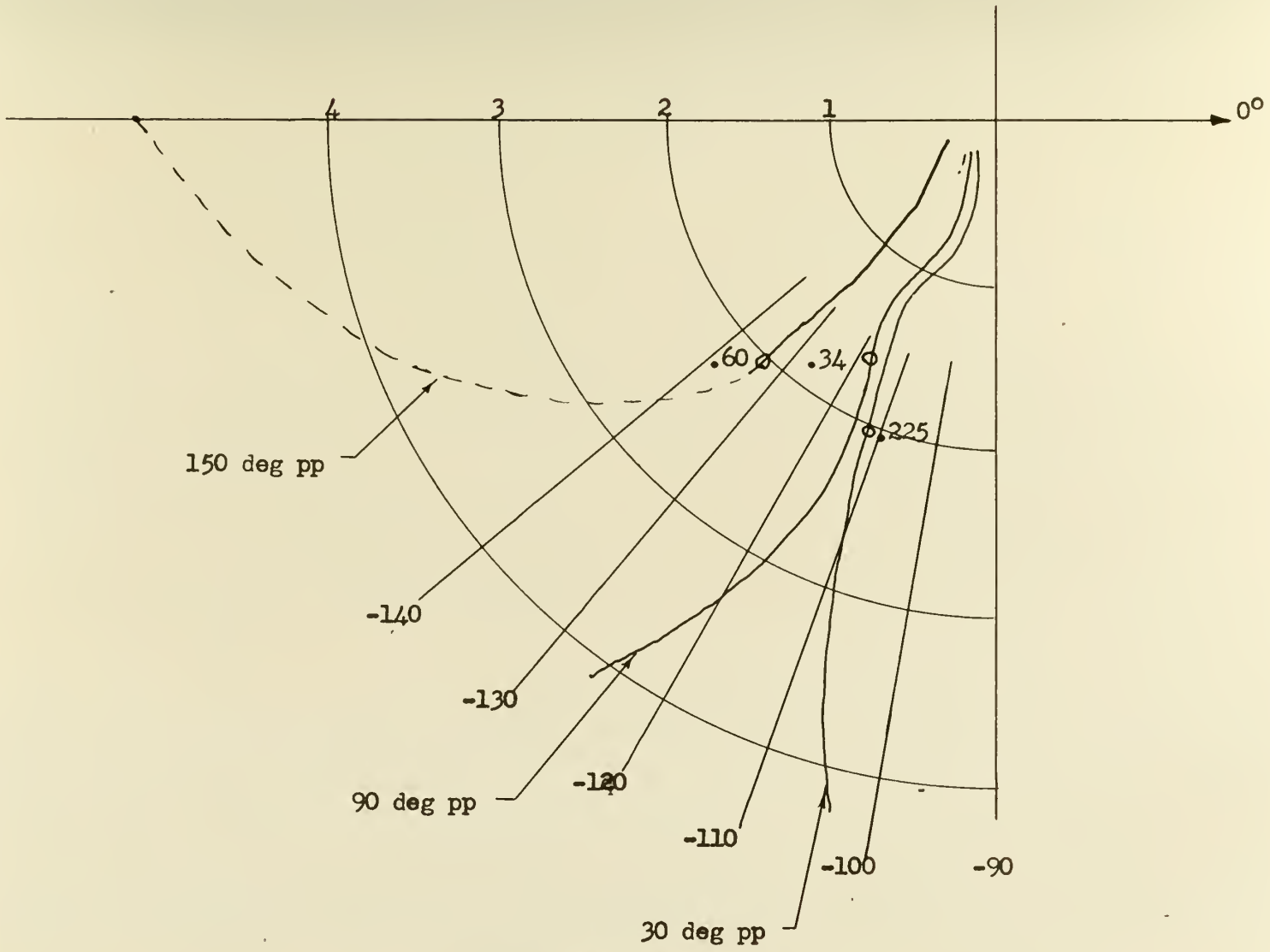

POLAR PLOT OF ERROR CONTROL
Figure 19

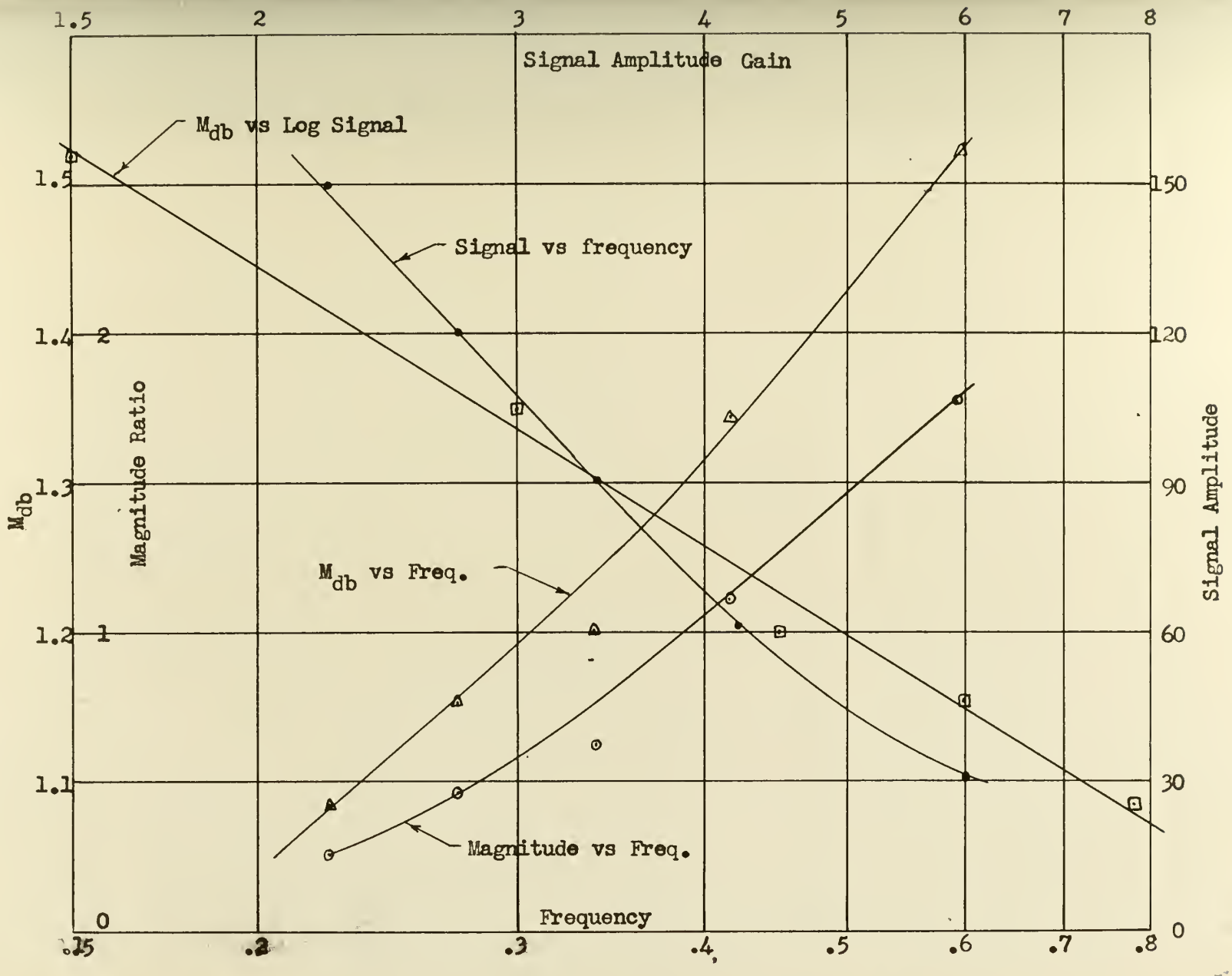

VARIATION OF RESONANT FREQUENCY AND MAGINTUDE
Figure 20

As signal amplitude is increased resonant frequency and magnitude both would be expected to decrease toward limits that are defined by velocity saturation of the system but this belies Equations (23) and (24). Which hypothesis is correct if either is yet to be shown.

Fig. 21 is a plot of the quotient of resonant magnitude divided by frequency of resonance vs. signal. The plot appears to be linear in semi-log coordinates indicating a logarithimic variation of the parameter with signal amplitude. The value of the plot is not apparent but it may be supposed that the zero signal intercept is of some significance.

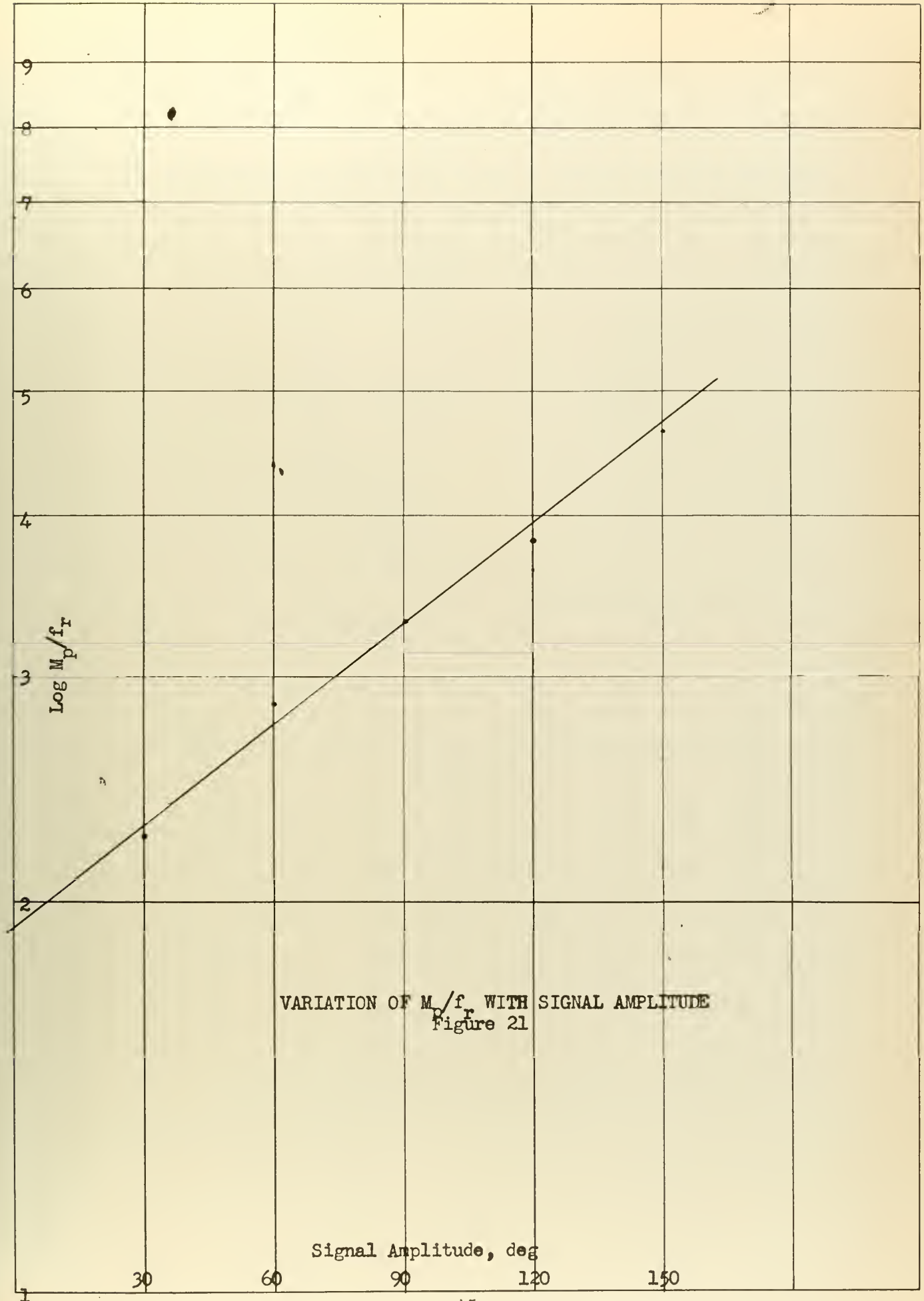

VARIATION OF M_p/f_r WITH SIGNAL AMPLITUDE
Figure 21

6. System Response to Error Plus Error Rate Control

The effect of adding error rate or derivative control to the system is to cause the switching lines to rotate from the vertical on the phase plane as is shown in Fig. 22.

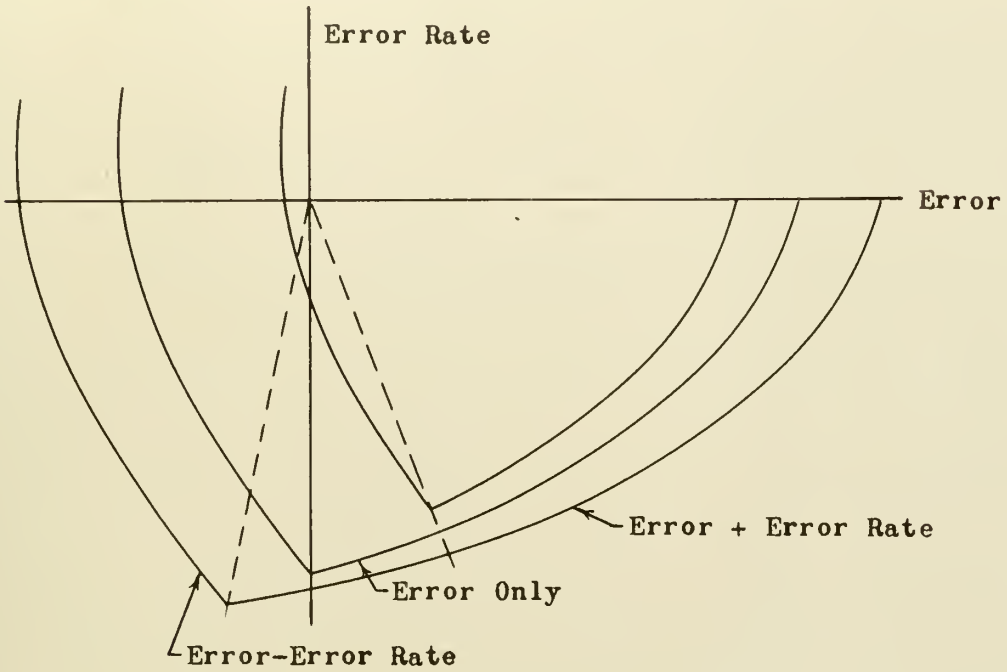

Effect & Error Rate Control on the Switching Lines
Figure 22

Reversal of the motor torque prior to reaching zero error allows the system to decelerate while it is still approaching the commanded position. This has the effect of reducing the overshoot and hence size of any limit cycle that might exist, thereby increasing the stability of the system, also reducing the settling-out time. The possibility exists that such control can give dead beat operation if the switch line can be made approximately parallel to the deceleration trajectory.

Error rate was added to the test system in increasing amounts until the switching lines had rotated counterclockwise to a position where the system commenced to step in toward the origin. The amount of error rate control that is added is herein defined as the ratio of error to error rate that is used to control; this is analogous to the slope deflection of the switching line from the vertical on the phase-plane. This may be conveniently expressed as a percent.

The effect of error rate control for one size step input is shown graphically in Fig. 23 where the system is stepping under 7.64% error rate control, dead beat for 6.11% and oscillatory for all lower amounts of error rate control. The corresponding transient responses are shown in Fig. 24 where the effect on the oscillatory nature of the system is more pronounced particularly in terms of peak overshoot. Percent peak overshoot appears to be approximately an inverse linear function of the amount of error rate control up to that amount necessary to make the system dead beat (Fig. 25), but this is for only one magnitude of step input and additional study is necessary to determine the true relationship.

Frequency response runs for a sampling of error rate control at one signal amplitude is shown in Fig. 26. It is noted that the resonant peaks all occur at the same frequency indicating that resonant frequency is not a function of the switching. This was checked at various signal amplitudes and found to be correct, i.e., resonant frequency is independent of switching control. The

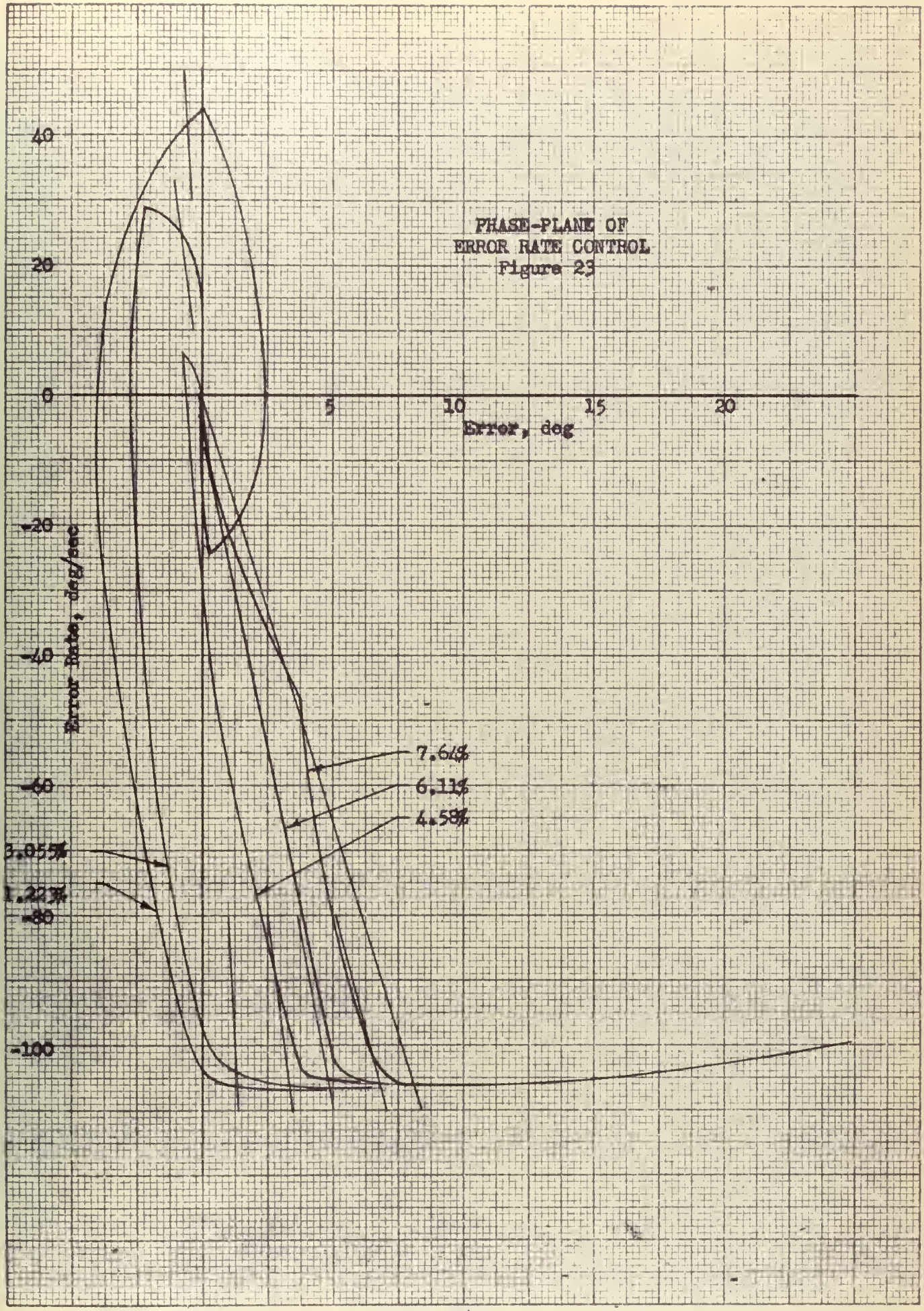

PHASE-PLANE OF
ERROR RATE CONTROL
Figure 23

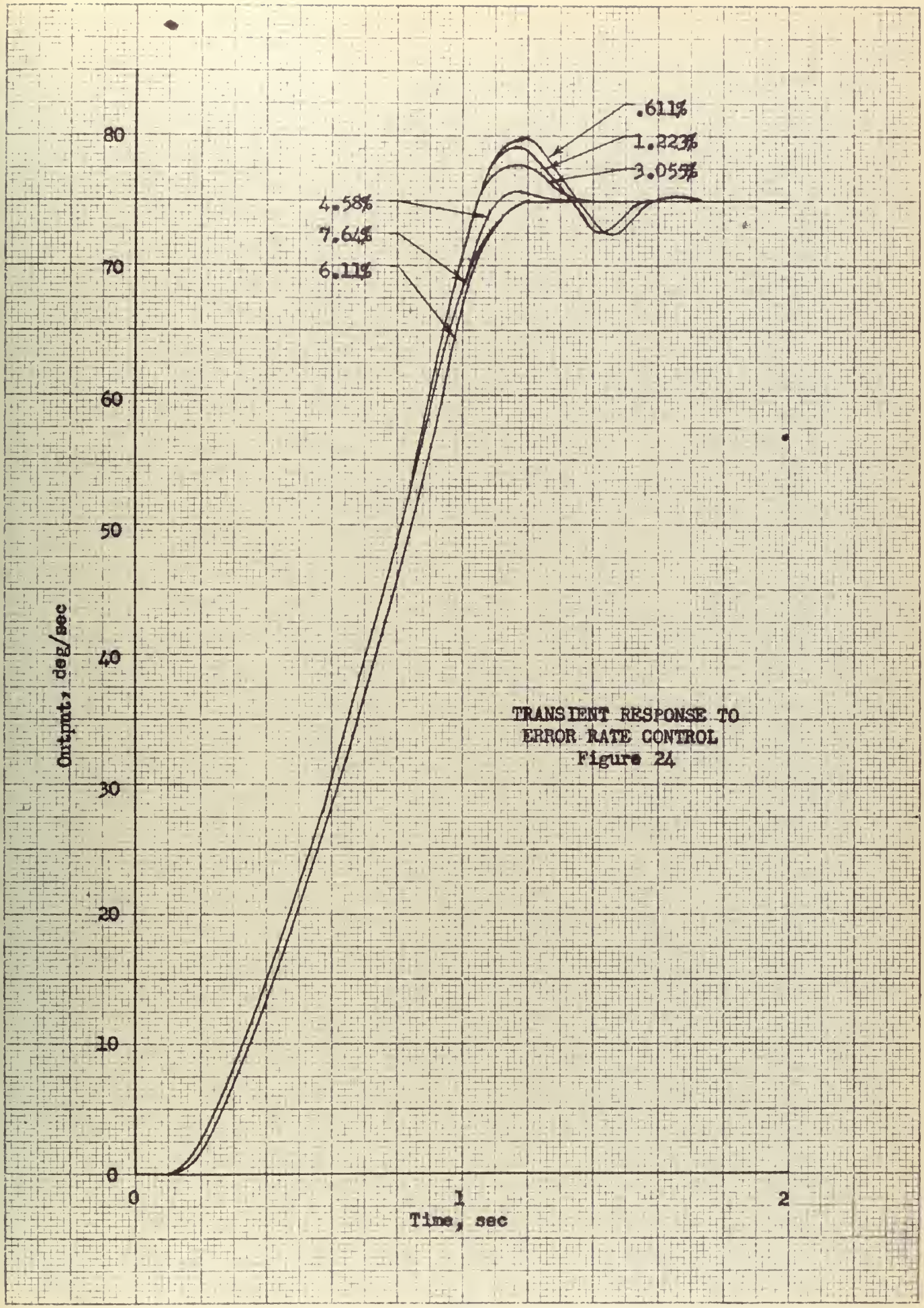

TRANSIENT RESPONSE TO
ERROR RATE CONTROL
Figure 24

THE EFFECT OF ERROR RATE CONTROL ON PEAK OVERSHOOT
Figure 25

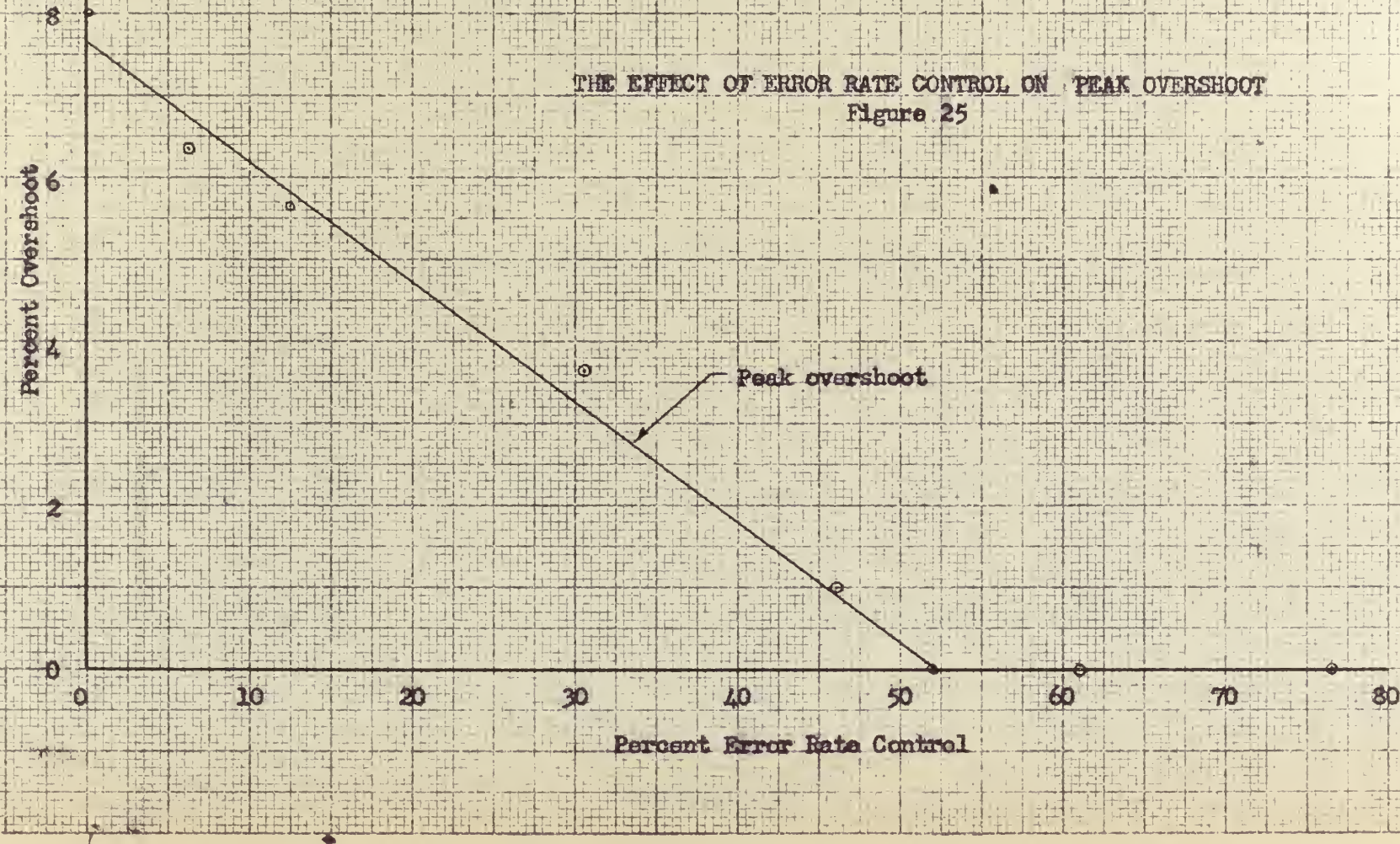

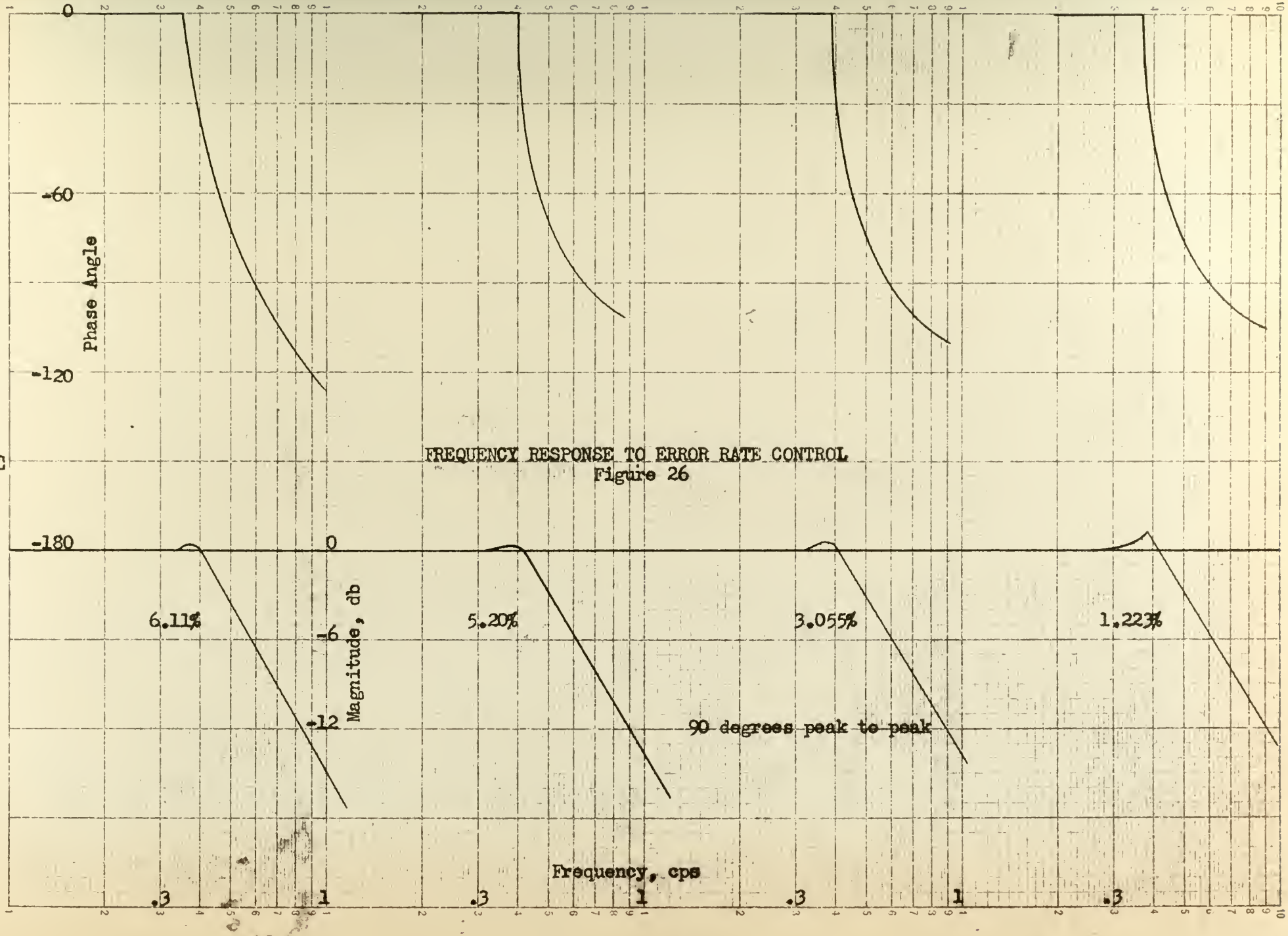

FREQUENCY RESPONSE TO ERROR RATE CONTROL
Figure 26

variation of resonant magnitude with error rate and signal amplitude is shown in Fig. 27, but these magnitudes are only slightly greater than unity and therefore not too significant.

The frequency response data was converted to open loop response curves via the M-N Contour Chart, Fig. 28. These are not only similar in shape as would be expected but are only slightly displaced from one another, thus error rate control affects the open loop response only slightly.

The magnitude curves of the open loop response shown in Fig. 29 are almost identical but the phase lag curves vary in shape. The slope of the magnitude curves is again about -48 db/octave reducing to -12 db/octave at a frequency slightly above that of the resonant peak. The point corresponding to the resonant peak appears highest on the magnitude curve for critical error rate control, that is the amount of control that will give dead beat operation. The phase angle peaks just after resonance and then drops off slowly in increasing amounts as error rate control is reduced. Phase margin is thus a slightly increasing function of error rate control, from 65^{o} to 75^{o} for the tests shown.

The polar plot (Fig. 30) indicates the similarity of the magnitude curves and shows the phase shift with error rate control. The variation in shape of the curves is thought to be due to measurement and data reduction rather than pecularities of the system because the form of control can only affect the time of relay action and has no effect on the power system whatever.

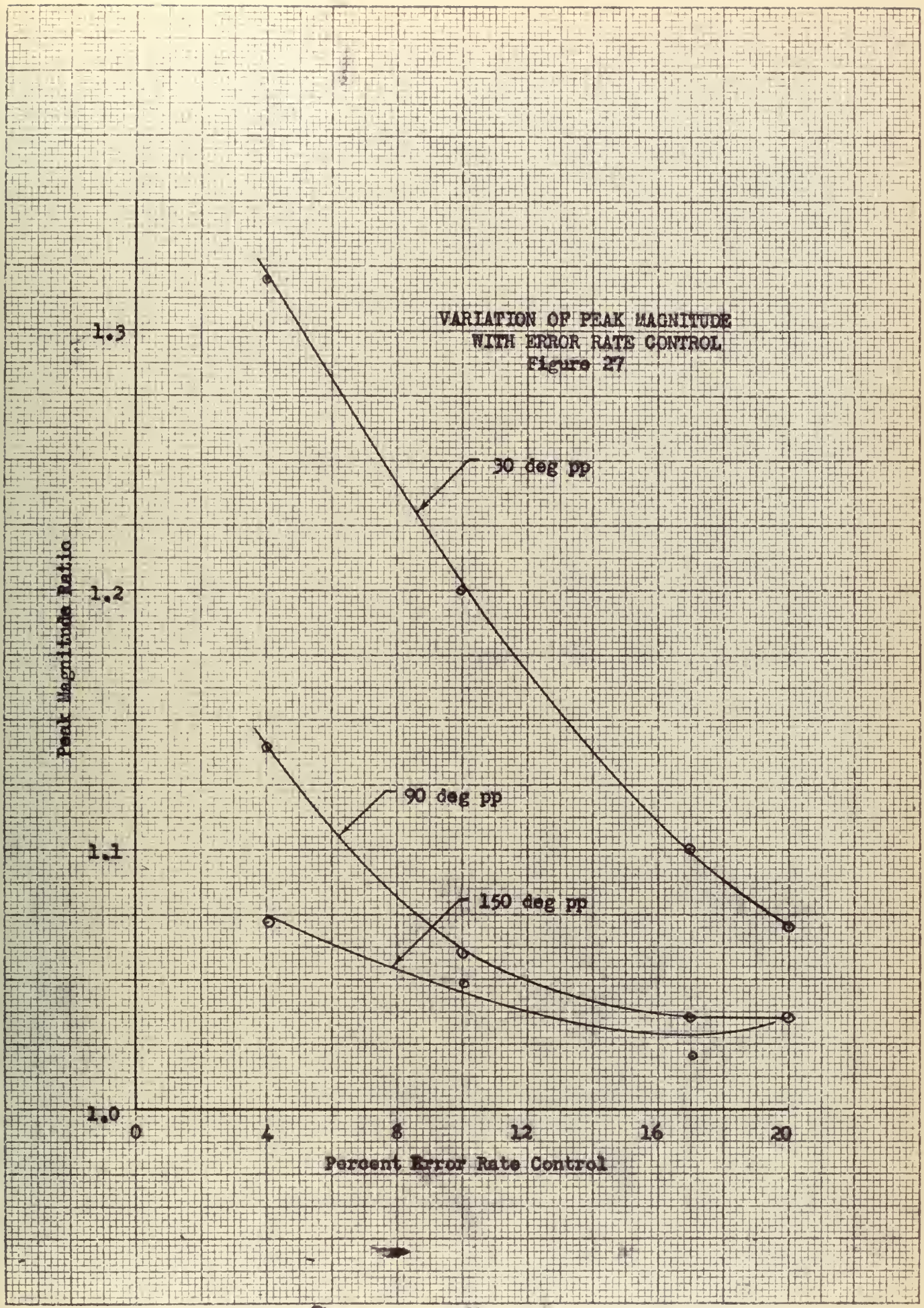

VARIATION OF PEAK MAGNITUDE
WITH ERROR RATE CONTROL
Figure 27

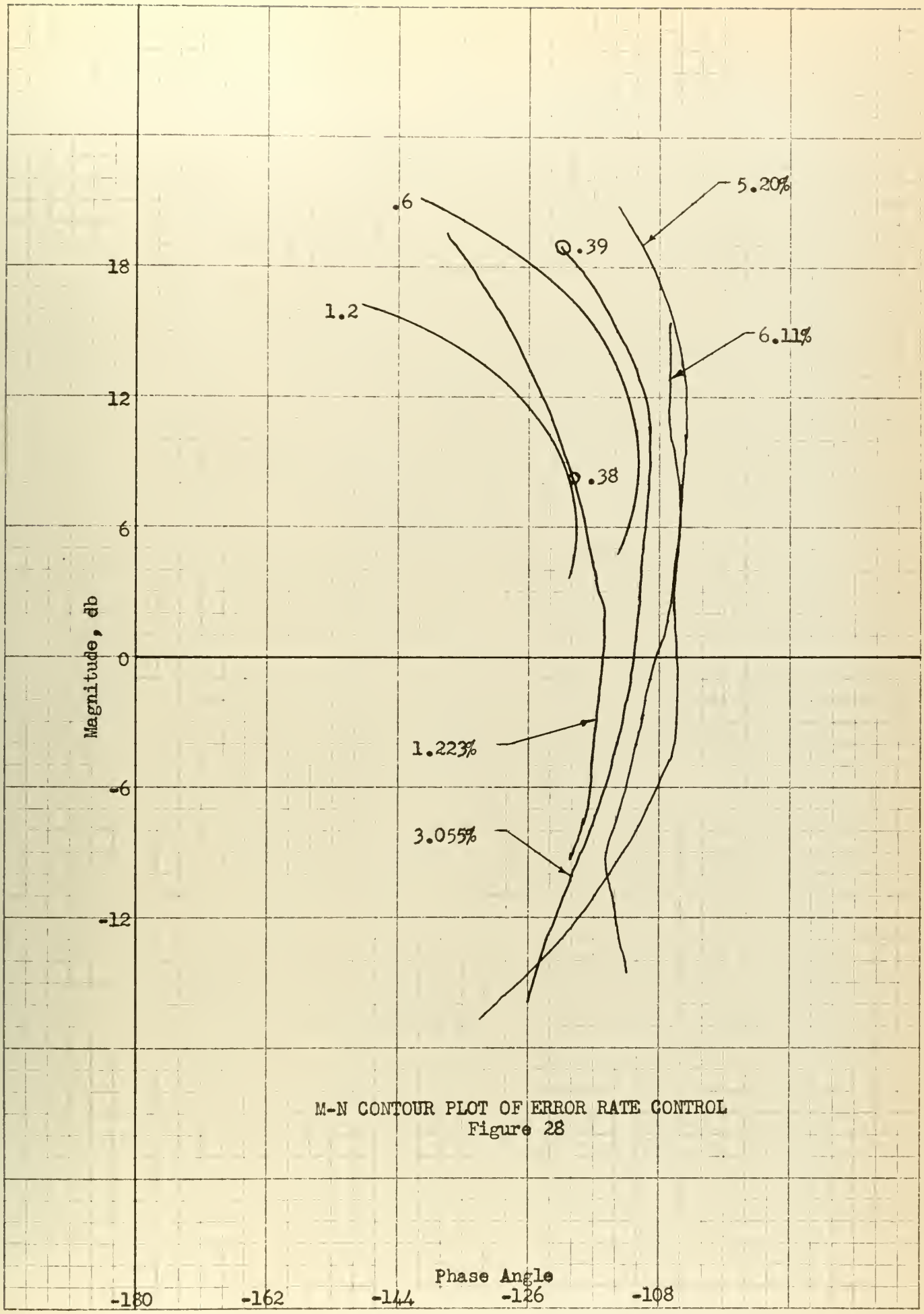

M-N CONTOUR PLOT OF ERROR RATE CONTROL
Figure 28

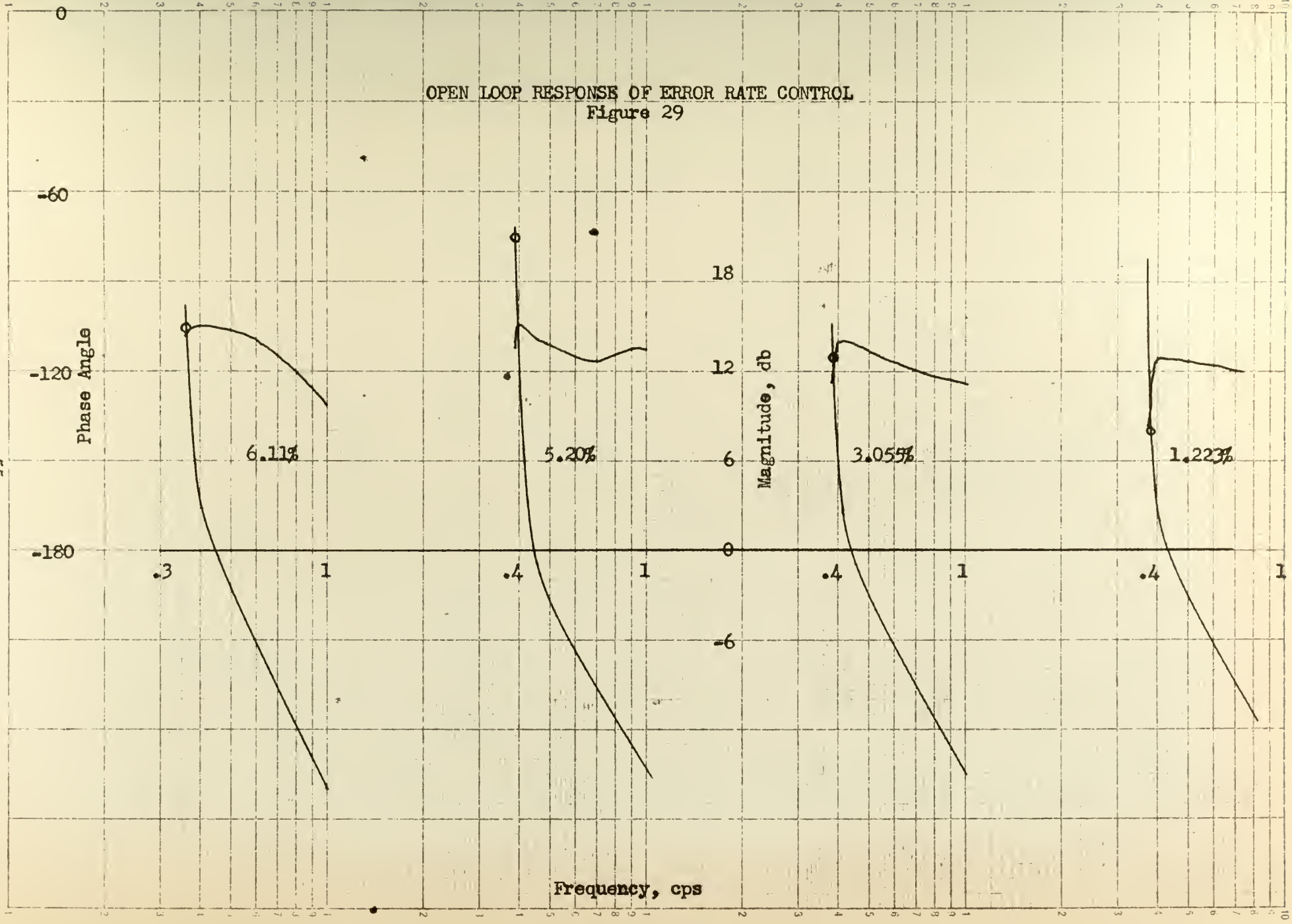
OPEN LOOP RESPONSE OF ERROR RATE CONTROL
Figure 29
0
-60
-120
-180
Phase Angle
18
12
6
0
-6
Magnitude, db
6.11%
5.20%
3.055%
1.223%
.3
1
.4
1
.4
1
.4
1
Frequency, cps

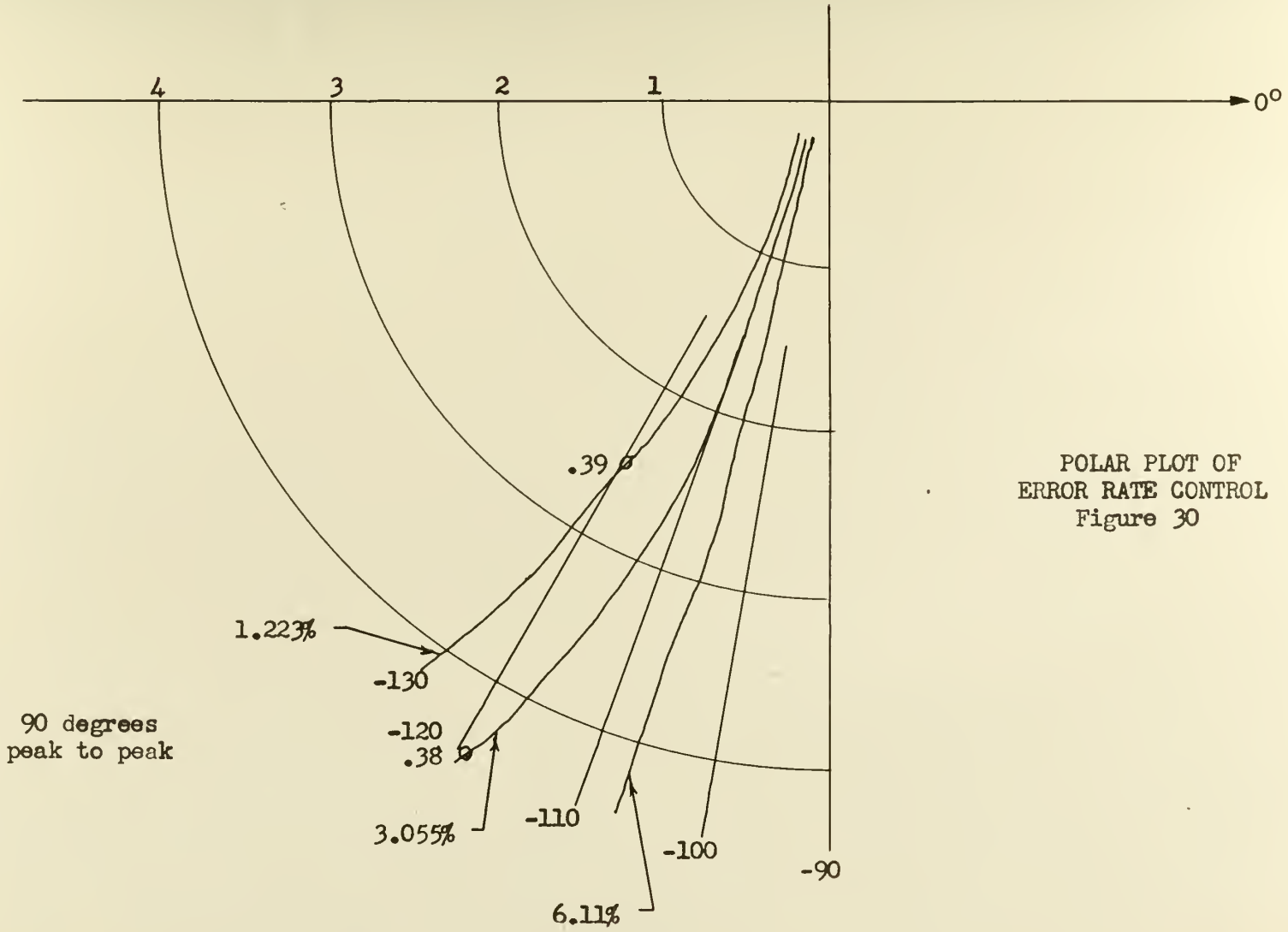

POLAR PLOT OF
ERROR RATE CONTROL
Figure 30

7. Optimized Control

The optimum relay servo as defined by Hopkin has proved to be difficult to attain. Hopkin described the system he used for experimental testing as one employing a curve fitting technique to attain optimum switching lines (4). This involved placing a template over the face of an oscilloscope, reading with a phototube the appearance of the trace beyond the template and using this information to cause switching to occur. This or some other complex procedure is required because the optimum switching lines are not straight but are complex curves to account for decelerating rates of most motors varying with initial velocity (1).

A variation of the optimum switching technique is that of dynamic braking or quasi-optimization. Instead of reversing the applied power at the switching line the motor terminals are shunted by a resistance, inductance or both and power is interrupted. The energy stored in the motor is discharged into the shunting element providing deceleration at a constant rate (15).

The motor under test was noted to have nearly straight line deceleration such as might be obtained with dynamic braking. This suggested the possibility of using derivative feedback to obtain a switching line along which the motor would track on reversal regardless of the signal amplitude. Fig. 31 shows the dead beat operation of the system for different amplitudes of step input controlled by error plus 5.20% derivative feedback. The system actually has reverse polarity power applied throughout the deceleration but the deceleration ratio so nearly matches the switching line that the

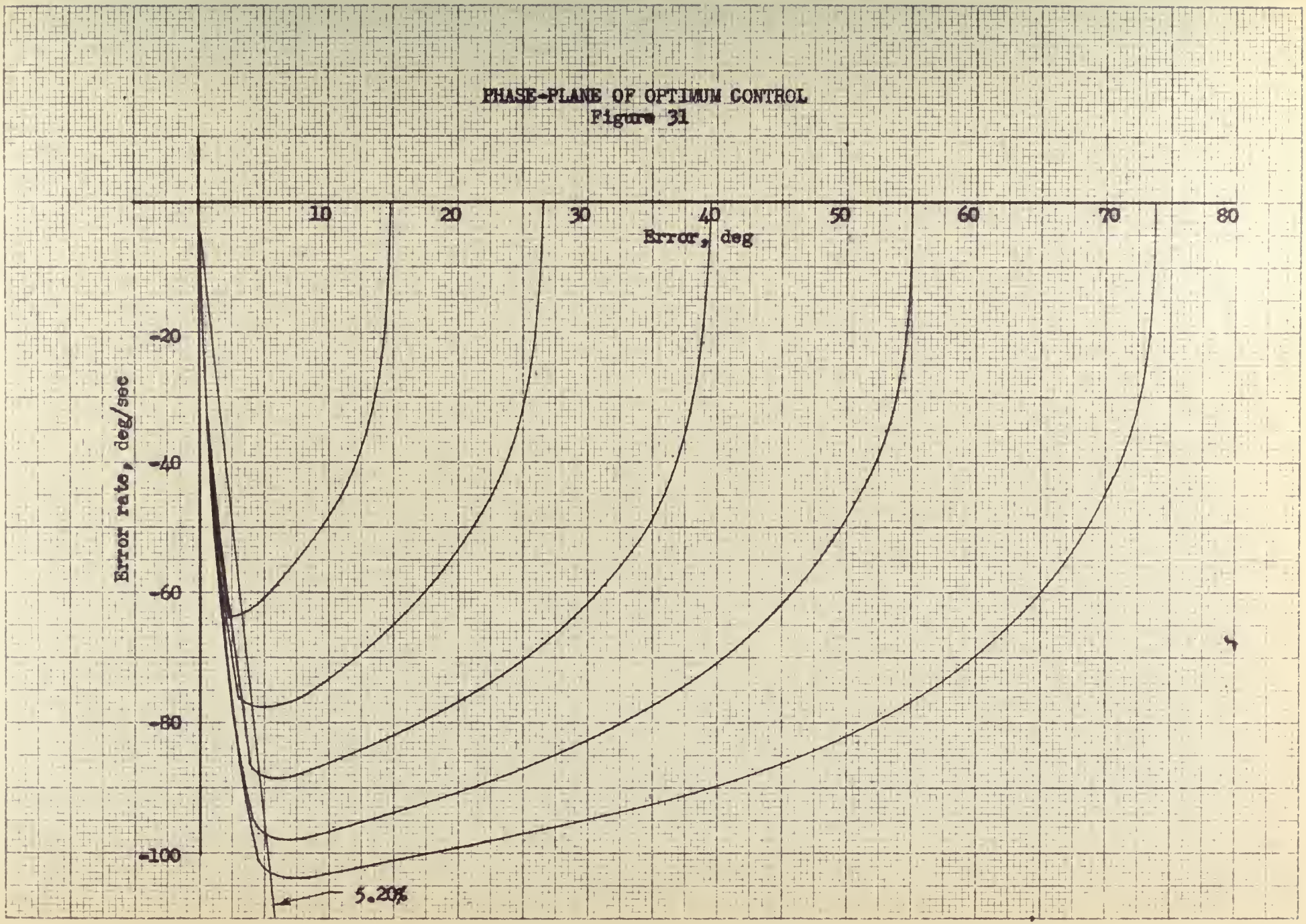
PHASE-PLANE OF OPTIMUM CONTROL
Figure 31
10
20
30
40
50
60
70
80
Error, deg
-20
-40
-60
-80
-100
Error rate, deg/sec
5.20%

system comes to rest within the one quarter of a degree dead zone of the relay. This system is not truly an optimum or quasi-optimum servo but somewhere in between since some dead zone is necessary to allow the system to dead beat. To prove this to be theoretically possible with an ideal relay would involve at least a complete general solution of the equations describing the system. Here indeed the template principle for drawing trajectories applies. The corresponding transients are shown in Fig. 32 and a comparison with Fig. 13 shows the system to dead beat in slightly over half the time the error controlled system takes to come to rest.

Frequency response for this optimized control is plotted in Fig. 33 for three amplitudes of signal. These appear not too different from those previously obtained except that the resonant peaks are quite small, of the order of .5 db.

Conversion to the open loop response through the use of the M-N contour charts (Fig. 34) provided the Bode Diagram, Fig. 35. The phase and magnitude curves are similar in shape but shifted in frequency and amplitude by the size of the input signal. The phase margin increase from 55^{o} to 80^{o} as the signal is increased fivefold. The similarity of the curves is shown in the polar plot, Fig. 36, where the curves appear to be rotated counterclockwise by signal amplitude.

Positioning servomechanisms requiring fast response and dead beat operation are complex and bulky because the performance requirements are conflicting in nature, requiring such a system to

TRANSIENT RESPONSE WITH OPTIMUM CONTROL
Figure 32

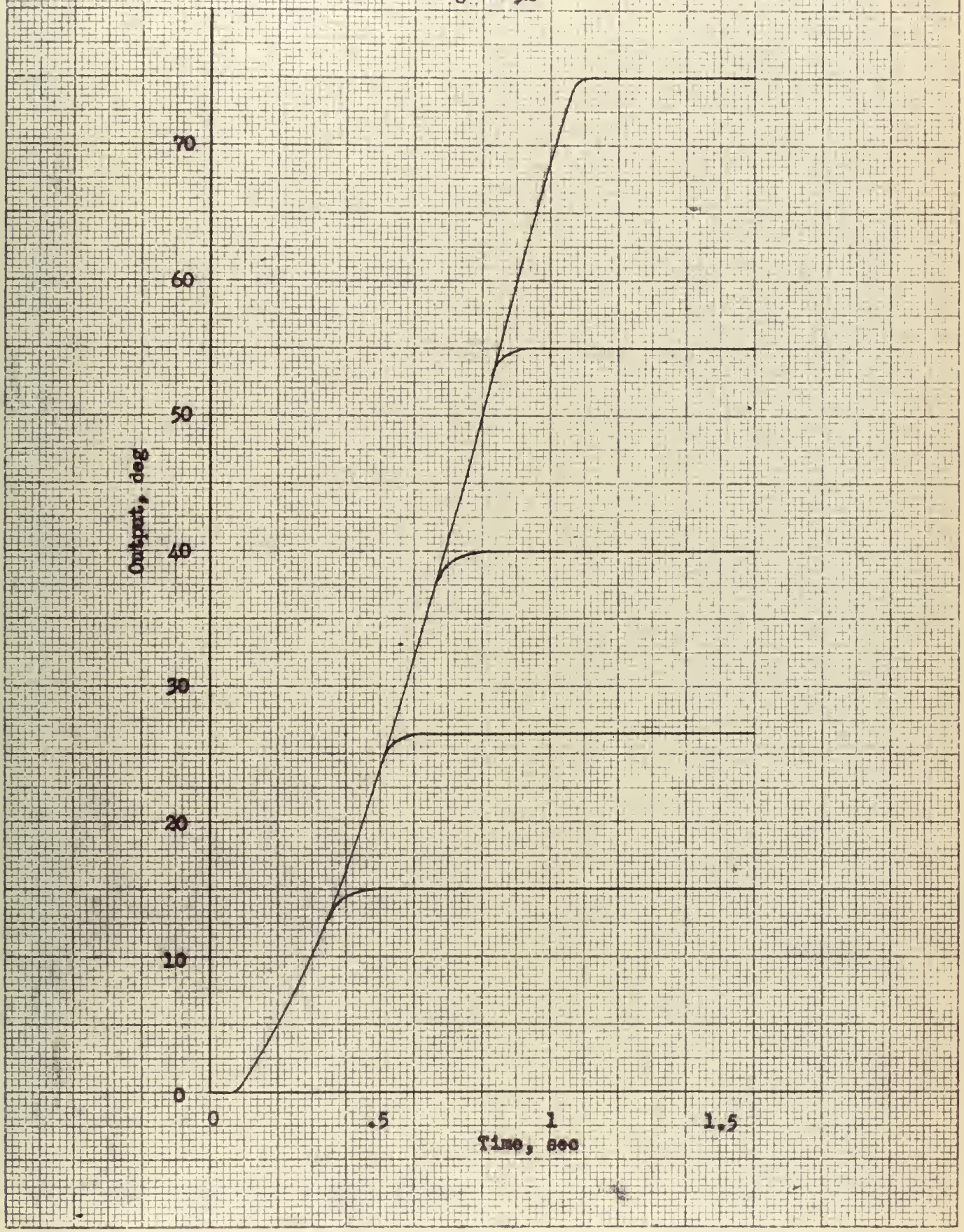

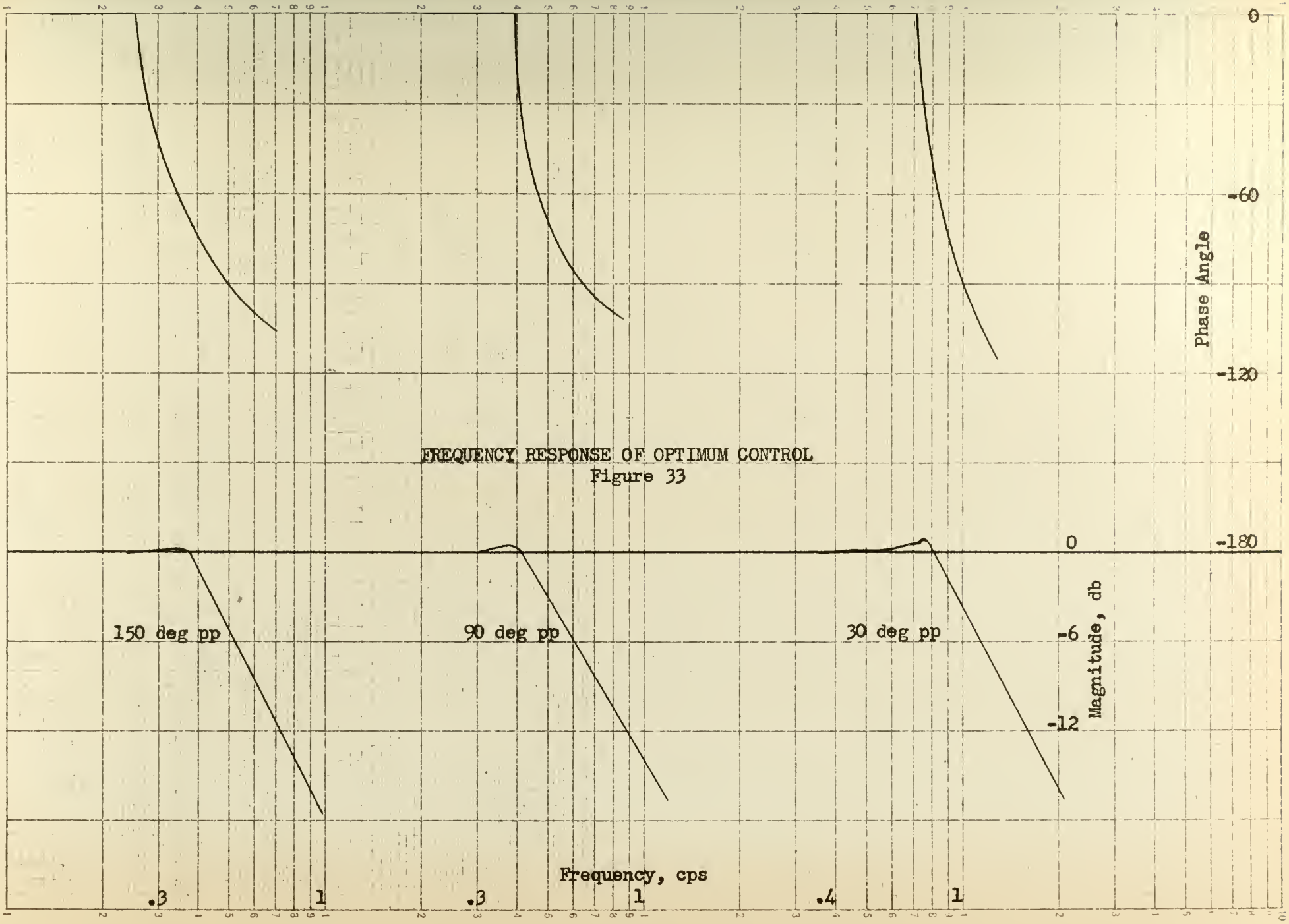

FREQUENCY RESPONSE OF OPTIMUM CONTROL
Figure 33

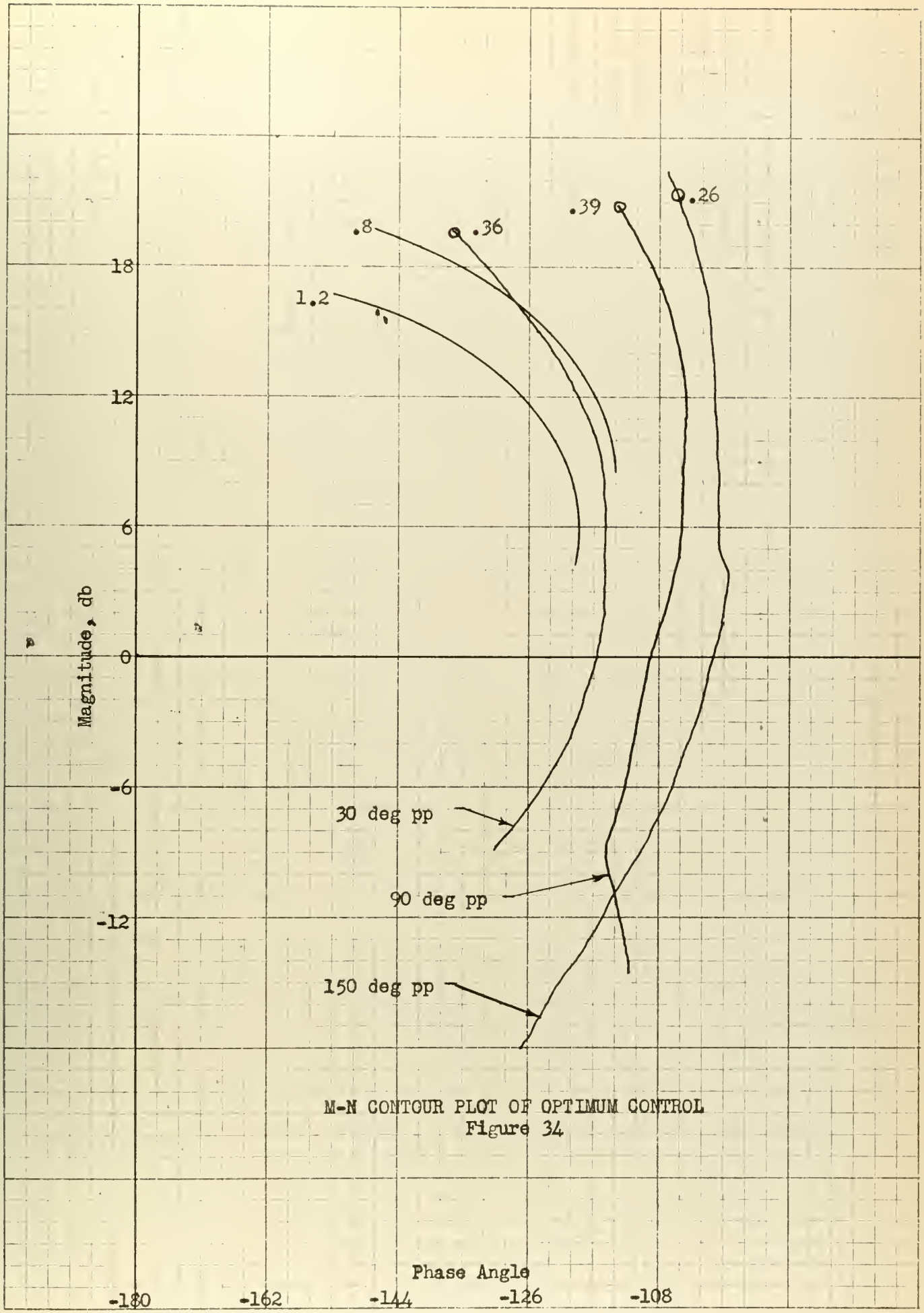

M-N CONTOUR PLOT OF OPTIMUM CONTROL
Figure 34

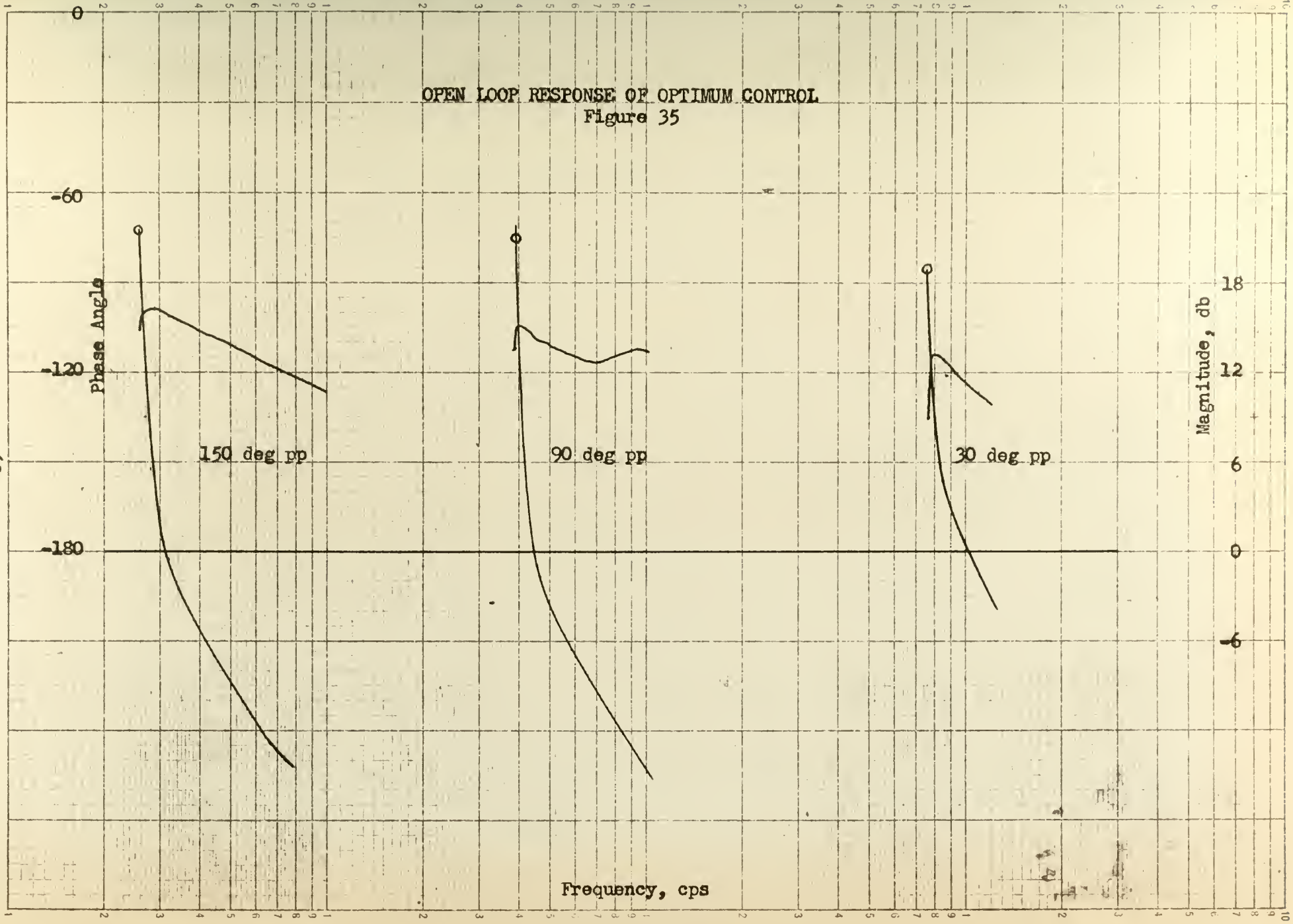
OPEN LOOP RESPONSE OF OPTIMUM CONTROL
Figure 35
0
-60
-120
-180
Phase Angle
150 deg pp
90 deg pp
30 deg pp
18
12
6
0
-6
Magnitude, db
Frequency, cps

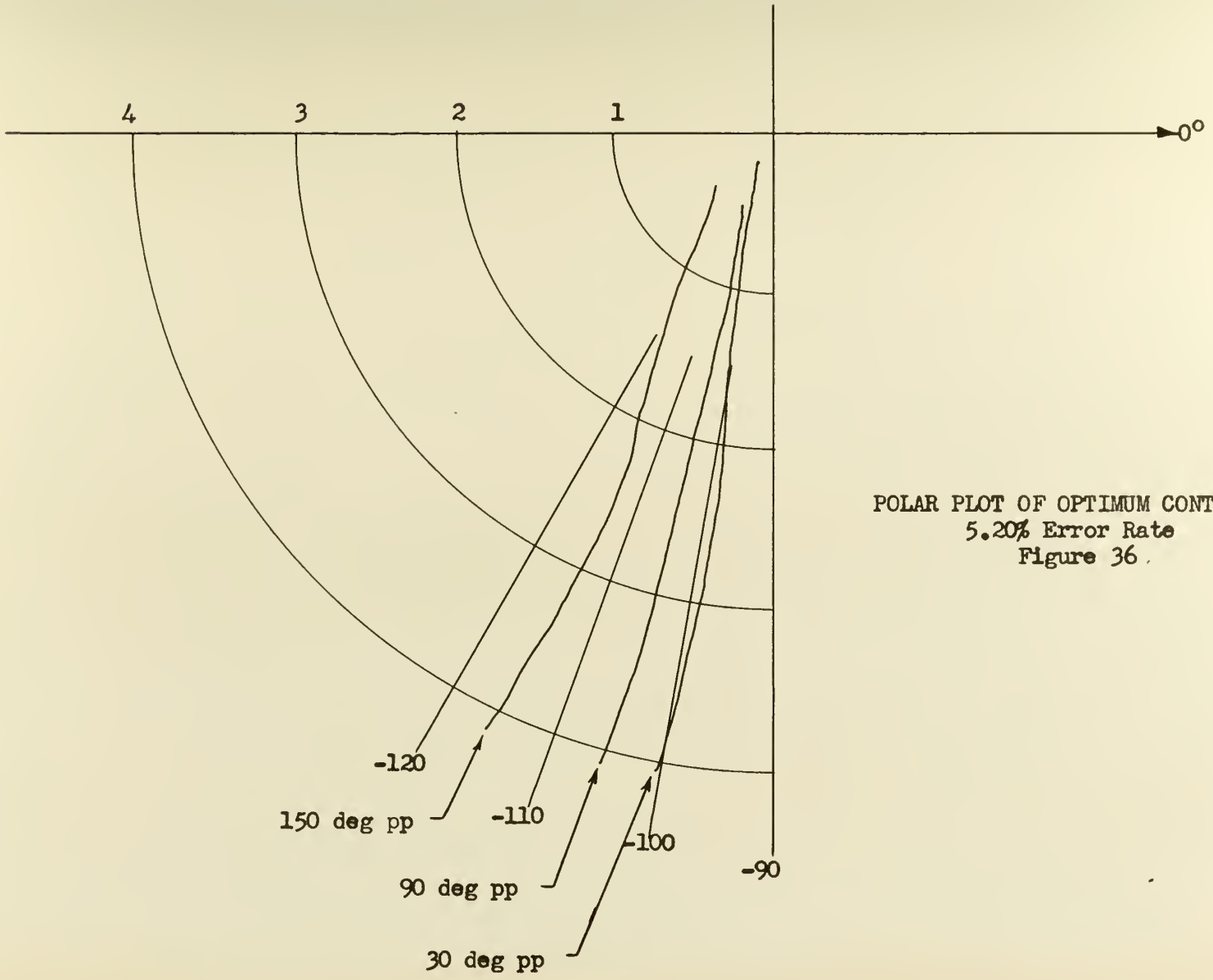

POLAR PLOT OF OPTIMUM CONTROL
5.20% Error Rate
Figure 36

employ non-linear feedback elements, complex compensation or be a dual mode system. If the split field series motor with simple derivative feedback giving optimum control can be exploited to satisfy the performance requirements then a great saving of weight, space, cost and increase in reliability may be realized. For these reasons continued study of the relay controlled split field series motor is justified, and since an a.c. series motor acts very much like its d.c. counterpart, an investigation into its characteristics in a relay system would also be of value.

8. The Effect of Inertia Loading

The addition of inertia to a system is expected to slow the response and cause the system to be more oscillatory in nature; to determine the effect of inertia on servo response an inertia disk was added to the motor shaft increasing the inertia of the system by 90%. The effect upon the transient response is evident when compared with the original response as shown in Fig. 37. The rise time is increased 30% which is roughly the square root of the ratio of total inertia. Only a slight increase in the tendency to oscillate is noticed however, only one more cycle being added indicating that the system stability is only slightly dependent upon inertia. Overshoot was increased by an amount almost in the same ratio as the ratio of total inertias. Settling-out time was roughly doubled.

A comparison of the two systems is presented in Fig. 38 in phase-plane form. The deceleration is not as sharp as in the original system but still quite rapid. The series motor is not nearly as adversely affected by inertia as are systems using other types of motors. It is also noted that there is a pronounced dissymmetry in the oscillations that must be attributed to differences in the two power channels, possibly in the relay control itself although the inductances of each winding are slightly different. Comparing the two systems under optimum derivative feedback control, Fig. 39, it can be seen that the larger inertia system has a more curving deceleration characteristic and would be more difficult to optimize for all amplitudes of signal. The amount of feedback necessary for

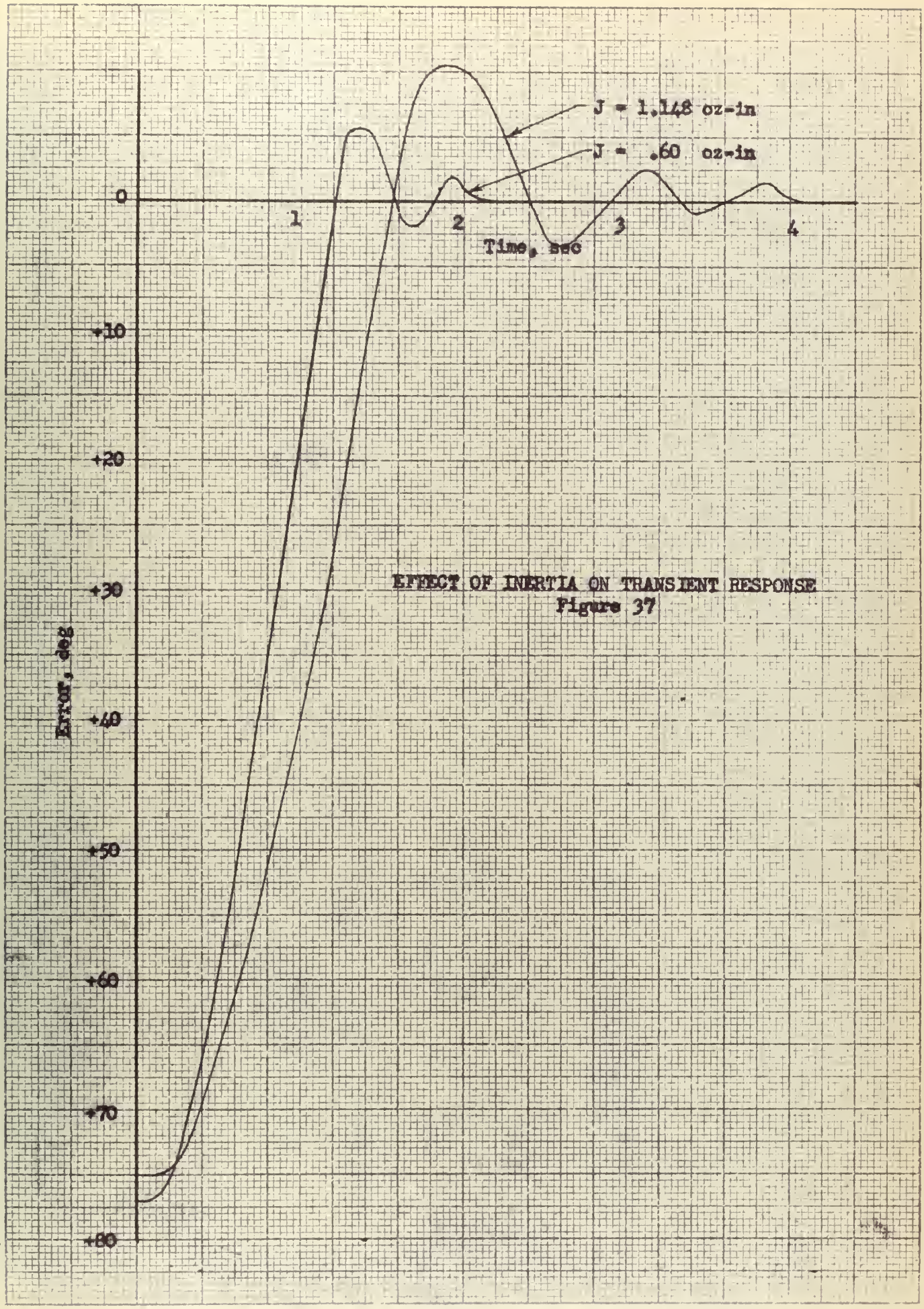

EFFECT OF INERTIA ON TRANSIENT RESPONSE
Figure 37

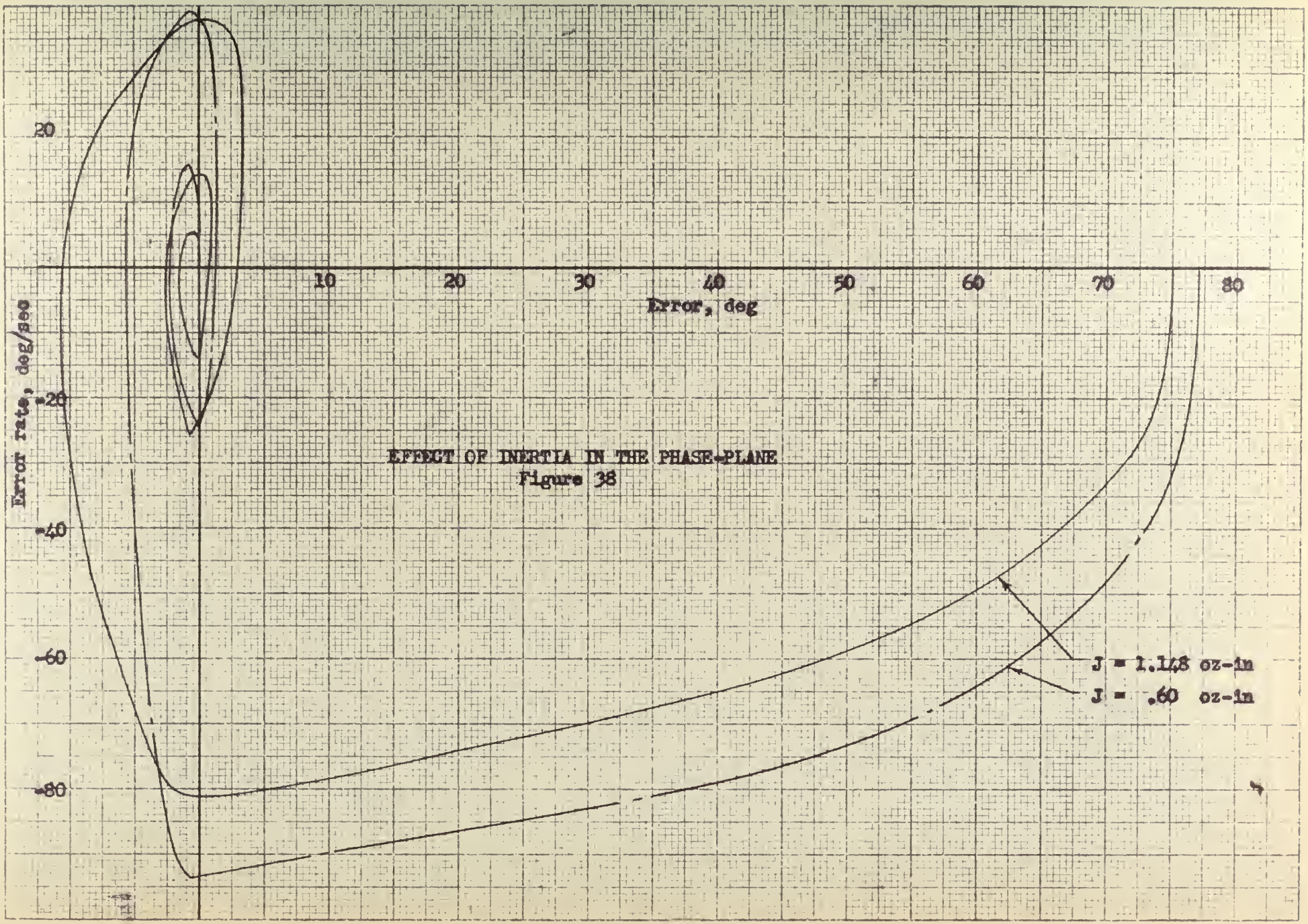

EFFECT OF INERTIA IN THE PHASE-PLANE
Figure 38

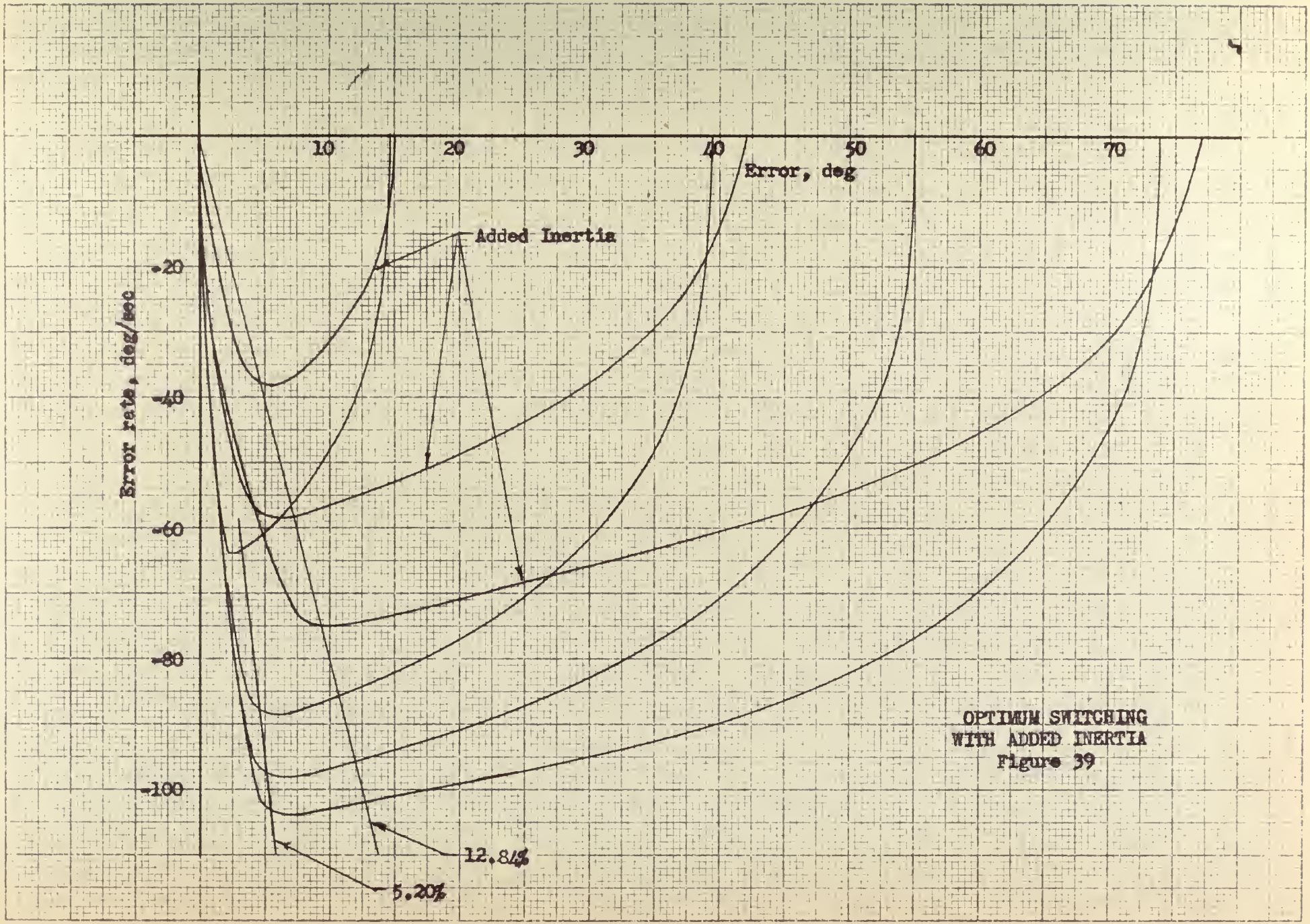

OPTIMUM SWITCHING
WITH ADDED INERTIA
Figure 39

optimizing would be increased due to the increased natural tendency to coast.

In general it appears that the error rate optimizing technique can be applied to series motor systems with wide limits on the system inertia.

9. System Response to a Relay with a Dead Zone

Since most relay systems employ relays of the electro-mechanical type and these have a finite dead zone, it was desirable to observe the system under these control characteristics. The dead zone was increased to 2.2°, this increased the dead zone at 100% power to 13° (See Fig. 12) thus above 6.5° deviation full power was available, partial power for error deviations between 1.1° and 6.5° and no power less than 1.1° deviation. The sloping character of the relay control lines appears to have little effect on the system response. The phase plane comparison of the switching action, Fig. 40, shows that switching occurs near or at the predicted switching lines and reversal action appears to be as positive as when the relay control lines were more nearly vertical.

The presence of dead zone increases the stability reducing the number of oscillations by allowing greater deviation of the rest position from the reference origin. The open dead zone also shows the character of the natural deceleration, viz., straight line deceleration due to viscous friction to a low value then coulomb friction hooks the curve into the rest position.

Here too is a clue to the amount of derivative feedback that is necessary for optimum deceleration. The slope for optimum control is shown to be nearly that of the natural deceleration due to viscous friction. The possibility exists that some torque is still being applied to the motor but since no stepping occurs in the deceleration curves for even the largest signal it is assumed that the energy stored in the motor is dissipated through the thyratrons

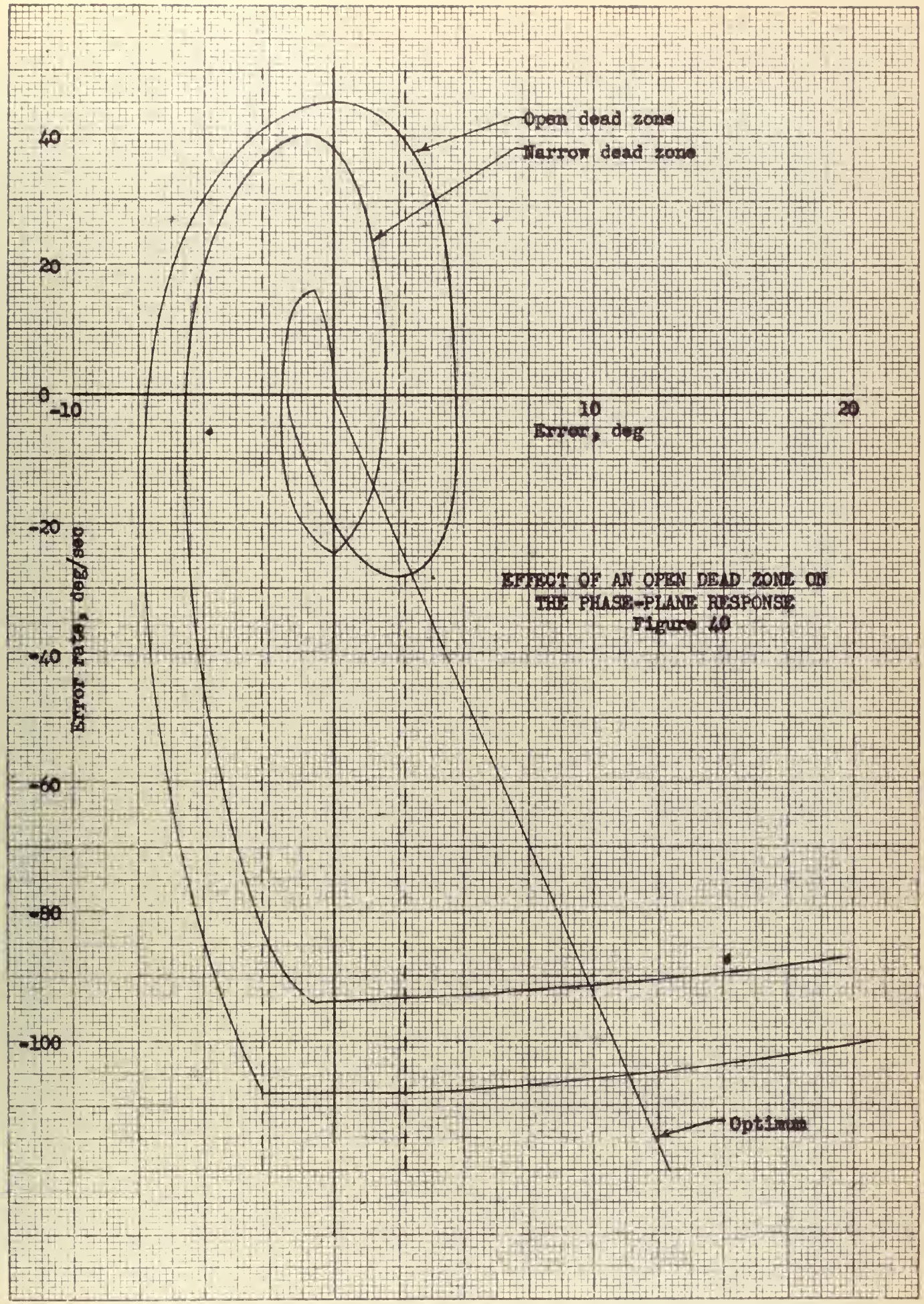

EFFECT OF AN OPEN DEAD ZONE ON THE PHASE-PLANE RESPONSE
Figure 40

in less than one half cycle thus extinguishing the tube before the a.c. anode supply swings positive again.

The change of transient characteristics is shown in Fig. 41 to be an enlargement of the oscillation until the system comes to rest within the dead zone both in magnitude and time. The lack of symmetry of the two power channels is evident here also in that the undershoot is almost as large as the overshoot. Optimum switching control is shown in the phase-plane of Fig. 42 again showing the natural deceleration to be very nearly parallel to the optimum switching lines.

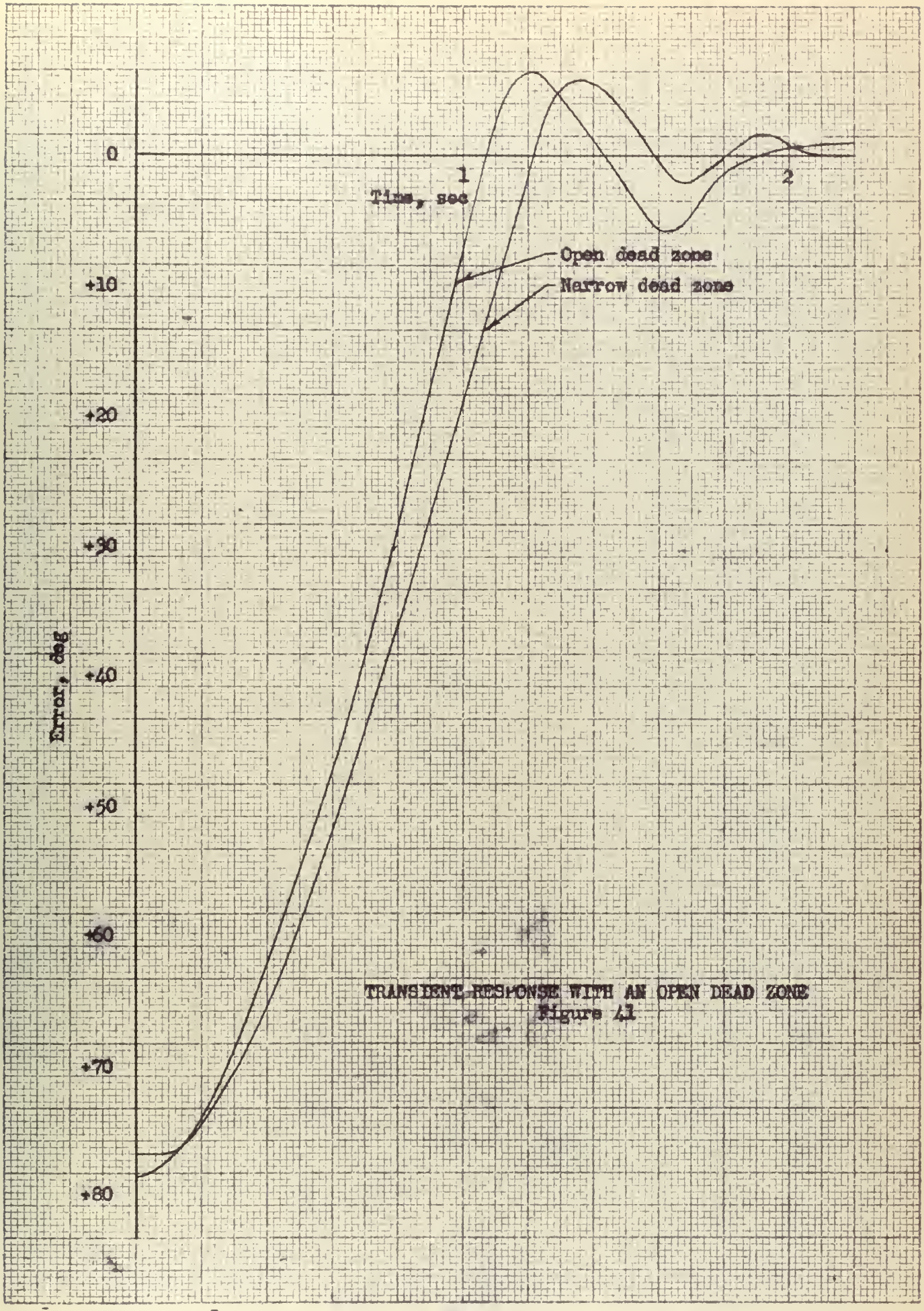

TRANSIENT RESPONSE WITH AN OPEN DEAD ZONE
Figure 41

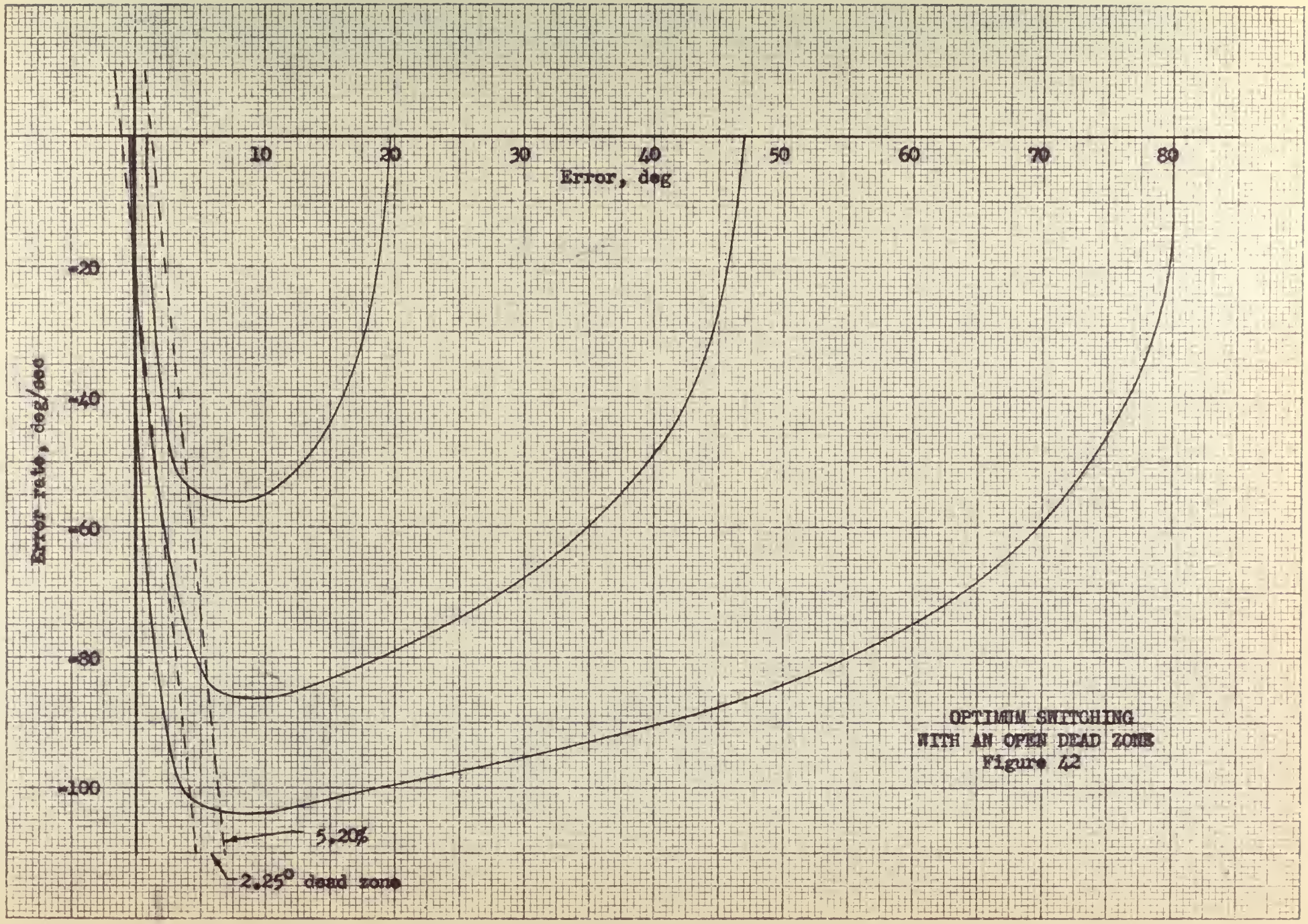

OPTIMUM SWITCHING
WITH AN OPEN DEAD ZONE
Figure 42

10. Summary and Discussion

The series motor produces torque proportional to the product of armature current and flux, and since flux is proportional to the armature current torque is proportional to the square of the current. This produces a high starting torque since current is limited only by the resistance and inductance of the motor until the back e.m.f. builds up as the motor velocity increases. When the motor is reversed the back e.m.f. becomes a negative voltage drop allowing an armature current much larger than the starting current to produce torque proportioned to its square thus causing a super-deceleration. As a result the system has a small overshoot and damps down to zero error very rapidly.

The system acts as if it were a "type 2" system in that the phase angle lags 180^{o} at very low frequencies. The polar plot of the open loop response remains entirely within the third quadrant until the gain is reduced to almost zero. The phase margin increases with signal amplitude but resonant frequency and bandwidth are reduced. The shape of the polar plots are quite similar for different signal amplitudes and appear only to be rotated counterclockwise by signal amplitude.

Error rate control provides earlier switching allowing the system to be decelerating while still approaching the origin. The deceleration curve is almost a straight line curved only slightly by high inertia loading allowing error rate switching to be used to optimize the response and achieve dead beat operation. The slope of the optimum switching line appears to be very nearly that

of natural deceleration but sufficient evidence to prove this is not available. The polar plots vary with error rate feedback as they do with signal amplitude, viz., rotate counterclockwise.

Tests of the system with open dead zone relay showed a lack of symmetry of action that was traced to the relay itself. The switching lines of the relay characteristics shown in Fig. 12 were found to increase their slopes asymmetrically. At the minimum dead zone setting used in most of the foregoing tests the sides were sloping but nearly identical. The fault lies in the grid control in that the action is not sufficiently sharp. What is needed in the snap action of a multivibrator and therefore such a control is recommended for any further study utilizing this relay rectifier. Fig. 43 is a proposed solution to the relay grid control problem. The multivibrator is an astable one-shot multivibrator plate coupled using a pentode and a triode. The triode is the normally-on tube and its plate is coupled to the screen of the pentode which is also used to control the action by the application of control signal. The pentode is driven at the grid by a rectified a.c. wave. The a.c. supply is the same as that of the gas tube anodes. A phase shifter provides the control necessary to obtain maximum conduction angle. The off-time of the triode must be adjusted to less than a half cycle and should be only large enough to fire the tube to avoid signal biasing of the thyratrons. This control has not been tested but is a fairly standard circuit and should provide snap action relay control.

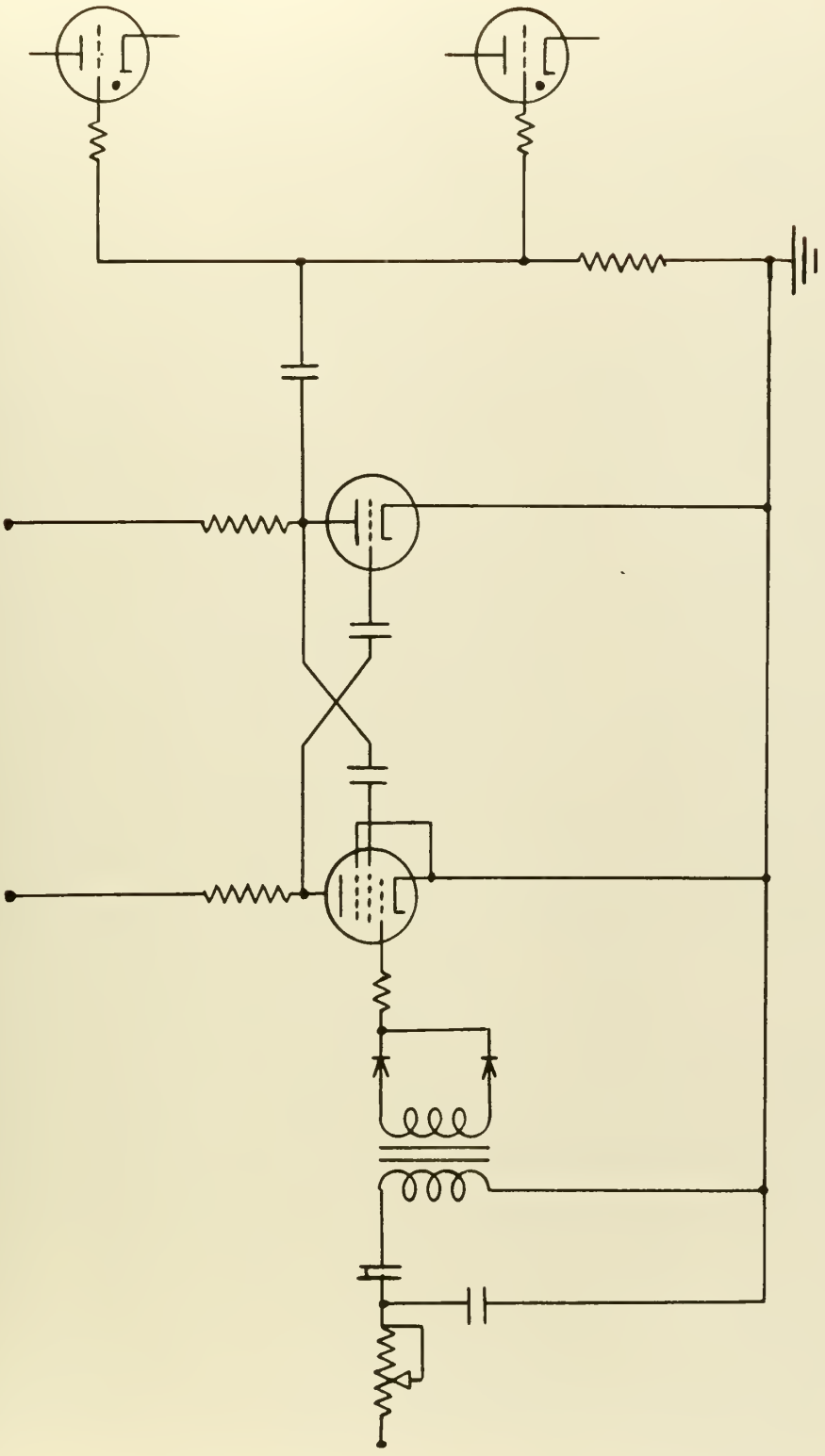

PROPOSED GRID CONTROL CIRCUIT
Figure 43

11. Conclusions and Recommendations

This study of a relay servo system using a split field series motor demonstrates several of the advantageous characteristics of system that could be exploited to reduce the cost, size and weight of many positioning servos that require high torque and fast response with or without dead beat operation.

It is concluded that:

1. The series motor produces torque proportional to the square of the armature current thus providing high torque for starting and even greater torque for reversal of direction.
2. The series motor is used in an error controlled relay servo system has a relatively fast response, a small overshoot and comes to rest with only a few oscillations.
3. The motor tested will come to rest within a relay dead zone of one quarter of a degree and will respond to command signals of less than one degree; therefore it is believed that the series motor system would respond to a true ideal relay with negligible limit cycling.
4. The deceleration curve of the system is very nearly a straight line allowing a linear switching line to provide very nearly optimum servo response for all magnitudes of step input. The linear switching line may be obtained by error plus error rate control of the relay.
5. The deceleration curves appear to be very nearly parallel to the natural deceleration curve due to viscous damping.

6. Bandwidth of the system is a decreasing function of signal amplitude while phase margin is an increasing one. Bandwidth and frequency of the resonant peak are independent of switching control but phase margin is an increasing function of error rate feedback.

7. The effect of inertia is to slow the response in both acceleration and deceleration, lower the stability slightly and increase the peak overshoot in proportion to the ratio of total inertias. Inertia increases the curvature of the deceleration curve only slightly thus allowing optimization to be obtained through wide limits of load inertia.

8. An open dead zone increases the system stability by allowing rest at a greater deviation from the commanded position.

It is recommended that further study be devoted to the following:

1. Continued study of this and other split field series motors to determining the variation of characteristics with the system parameters particularly with respect to optimum relay control. The effects of viscous friction, motor voltage, inertia and dead zone should be thoroughly investigated. Operation using electromechanical relays should be examined to determine the effect of unequal pull-in and drop-out points on the response.

2. The a.c. series motor should be studied to determine its application in relay servomechanisms.

3. A study of the general computer solution of the split field series motor would allow a great deal of parameter investigation to

be accomplished synthetically.

4. Continued effort be applied toward an analytical solution of the system.

REFERENCES AND BIBLIOGRAPHY

1. Thaler, G. J.; Unpublished notes on Non-Linear Servomechanisms

2. Hazen, H. L.; Theory of Servo-Mechanisms, Journal of the Franklin Institute, Vol. 218, No. 3, pp. 279-331, Sept. 1934

3. Weiss, H. K.; Analysis of Relay Servomechanisms, Journal of Aeronautical Sciences. Vol. 13, No. 7, pp. 364-376, July 1946

4. Hopkin, A. M.; "A Phase-Plane Approach to the Compensation of Saturating Servomechanisms", A.I.E.E. Transactions, Vol. 10, Part I, pp. 631-9, 195

5. Goldfarb, L. C.; "On Some Non-Linear Phenomena in Regulatory Systems," Avtomatika i Telemekhanika, Vol. 8, No. 5, Sept.-Oct., 1947, pp. 349-383 (Russian) as Translated in National Bureau of Standards Report 1691, 1952

6. Lechtman, E. Y.; "On the Computation of Relay Servo-Mechanisms," Avtomatika i Telemeklanika, Vol. 12, No. 1, Jan.-Feb., 1951, pp. 15-27 (Russian). Translated in National Bureau of Standards Report 1691, 1952.

7. Chestnut, H.; Mayer, R. W.; Servomechanism and Regulating System Design, Vol. II, pg. 223, John Wiley & Sons, Inc., New York, 1955

8. Williams, A. J., Jr.; "Combined Thyratron and Tachometer Speed Control of Small Motors," A.I.E.E. Transactions, Vol. 57, pp. 565-8, 1938

9. Ware, L. A.; "Water Level Indicator," Electronics, Vol. 13, pp. 23-5, 1940

10. Lear, W. P.; "Remote and Automatic Electric Control for Aircraft," Journal of the Franklin Institute, Vol. 238, No. 1, pp. 9-35, July, 1944

11. Hale, H. Erwin; "The K-8 Computing Gunsight," Electronics, Vol. 18, No. 1, pp. 94-9, Jan. 1945

12. Fry, Macon; "Designing Computing Mechanisms. Part VI-Servomechanism," Machine Design. Vol. 18, No. 1, pp. 115-118, Jan. 1946

13. Rothauge, C. H., Thaler, G. J.; Unpublished notes on Electrical Transients.

14. Thaler, G. J., Stein, W. A.; Transfer Function and Parameter Evaluation for D-C Servomotors, A.I.E.E. Transaction, Part II, pp. 410-17, Jan. 1946

15. Harris, W. L., Jr., McDonald, C., Thaler, G. J.; "Quasi-Optimumization of Relay Servos by Use of Discontinuous Damping." A.I.E.E. Transactions Part II, pp. 292-6, Nov. 1957

thesG58
Investigation of a relay servo using a s
3 2768 001 03526 4
DUDLEY KNOX LIBRARY